

**STRUCTURAL AND ELLIPSOMETRIC PROPERTIES OF GaS(x)Se(1-x)
LAYERED MIXED CRYSTALS**



A MASTER'S THESIS

in

Applied Physics

AtIhm University

by

OM-ALHANA HABAIBI

NOVEMBER 2017

**STRUCTURAL AND ELLIPSOMETRIC PROPERTIES OF GaS(x)Se(1-x)
LAYERED MIXED CRYSTALS**

**A THESIS SUBMITTED TO
THE GRADUATE SCHOOL OF NATURAL AND APPLIED SCIENCES
OF
ATILIM UNIVERSITY
BY
OM-ALHANA HABAIBI**

**IN PARTIAL FULFILLMENT OF THE REQUIREMENTS FOR THE
DEGREE OF**

MASTER OF SCIENCE

IN

THE DEPARTMENT OF APPLIED PHYSICS

NOVEMBER 2017

Approval of the Graduate School of Natural and Applied Sciences, Atılım University.

Prof. Dr. Ali Kara

Director

I certify that this thesis satisfies all the requirements as a thesis for the degree of Master of Science.

Prof. Dr. Ramazan Aydın

Head of Department

This is to certify that we have read the thesis “STRUCTURAL AND ELLIPSOMETRIC PROPERTIES OF GaS(x)Se(1-x) LAYERED MIXED CRYSTALS” submitted by “OM-ALHANA HABAIBI” and that in our opinion it is fully adequate, in scope and quality, as a thesis for the degree of Master of Science.

Assoc. Prof. Dr. Filiz Korkmaz Özkan
Co-Supervisor

Assoc. Prof. Dr. Mehmet Işık
Supervisor

Examining Committee Members

Prof. Dr. Nizami Hasanli

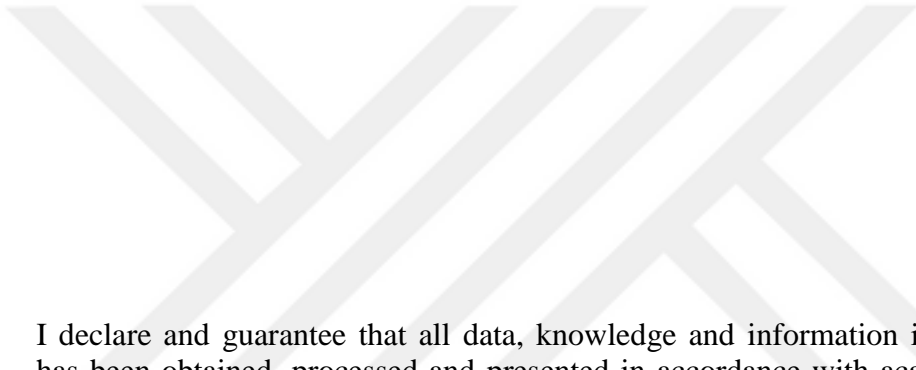
Prof. Dr. Ramazan Aydın

Assoc. Prof. Dr. Kemal Efe Eseller

Assoc. Prof. Dr. Mehmet Işık

Assoc. Prof. Dr. Filiz Korkmaz Özkan

Date: 23.11.2017



I declare and guarantee that all data, knowledge and information in this document has been obtained, processed and presented in accordance with academic rules and ethical conduct. Based on these rules and conduct, I have fully cited and referenced all material and results that are not original to this work.

Name, Last name: OM-ALHANA HABAIBI

Signature:

ABSTRACT

STRUCTURAL AND ELLIPSOMETRIC PROPERTIES OF GaS(x)Se(1-x) LAYERED MIXED CRYSTALS

Habaibi, Om-Alhana

M.S., Applied Physics Department

Supervisor: Assoc. Prof. Dr. Mehmet Işık

Co-Supervisor: Assoc. Prof. Dr. Filiz Korkmaz Özkan

November 2017, 48 pages

GaS_xSe_{1-x} layered mixed crystals were investigated using structural and optical characterization techniques. Structural characterization of samples grown by Bridgman method were accomplished using x-ray diffraction (XRD), energy dispersive spectroscopy (EDS) and fourier transform infrared (FTIR) spectroscopy techniques. Compositional dependence of mixed crystals were obtained from EDS experiments. Results of measurement indicated that used samples correspond to composition of x varying from 0 to 1 by 0.25 intervals. The crystal structures of the samples were revealed using the results of XRD measurements and a software program for analyses. FTIR spectra of the samples indicated the presence of multiphonon absorptions in the samples for compositions of $x = 0, 0.25$ and 0.50 . The results of XRD and FTIR experiments were associated between the used compositions.

Optical characterization of the samples were achieved by ellipsometry experiments carried out in the spectral range of 1.2-6.0 eV. The output data of measurement system were converted to data presenting the spectral dependency of optical parameters. Ellipsometric data was used to obtain the band gap energy of the samples. Obtained band gap energy values showed that as sulfur composition is increased in the mixed crystals, band gap energy increases from 2.04 eV ($x = 0$) to

2.57 eV ($x = 1$). According to revealed band gap energy values, a graph presenting the compositional dependence of bang gap energy was plotted.

Keywords: GaSe, GaS, Ellipsometry, Layered crystals, Structural properties



ÖZ

GaS(x)Se(1-x) KATMANLI KARIŞIM KRİSTALLERİNİN YAPISAL VE ELİPSOMETRİK ÖZELLİKLERİ

Habaibi, Om-Alhana

Yüksek Lisans, Uygulamalı Fizik Bölümü

Tez Yöneticisi: Doç. Dr. Mehmet Işık

Ortak Tez Yöneticisi: Doç. Dr. Filiz Korkmaz Özkan

Kasım 2017, 48 sayfa

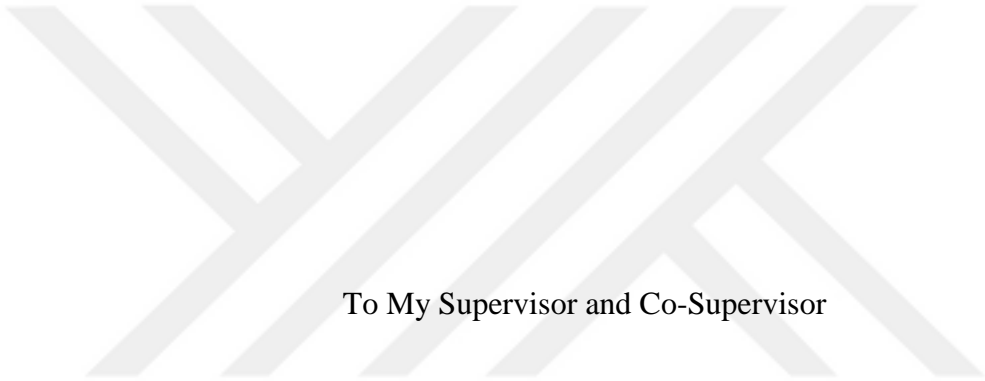
GaS_xSe_{1-x} katmanlı karışım kristalleri yapısal ve optiksel karakterizasyon teknikleri kullanılarak incelendi. Bridgman metodu ile büyütülen örneklerin yapısal karakterizasyonu x-ışını kırınımı (XRD), enerji saçılım spektroskopisi (EDS) ve Fourier transform kızılötesi spektroskopisi teknikleri kullanılarak başarıldı. Karışım kristallerinin kompozisyonel bağımlılığı EDS deneyleri ile elde edildi. Ölçümlerin sonuçları, kullanılan örneklerin x değerinin 0.25 aralıklar ile 0 ile 1 arasında olduğu kompozisyona denk geldiğini gösterdi. Örneklerin kristal yapısı XRD ölçümlerinin sonuçlarını ve analiz için bir yazılım programı kullanarak açığa çıkarıldı. FTIR tayfları x=0, 0.25 ve 0.50 kompozisyonlarındaki örneklerin içerisinde çoklu fonon emiliminin var olduğunu gösterdi. XRD ve FTIR deneylerinin sonuçları kullanılan kompozisyonlar arasında ilişkilendirildi.

Örneklerin optiksel karakterizasyonu 1.2-6.0 eV spektral aralığında gerçekleştirilen elipsometri deneyleri ile tamamlandı. Ölçüm sisteminin çıkış datası optiksel parametrelerin spektraş bağımlılığını gösteren dataya çevrildi. Elipsometrik data örneklerin bant boşluğu enerjilerini elde etmek için kullanıldı. Elde edilen bant enerjisi değerleri karışım kristallerinde sülfür kompozisyonu arttıkça bant enerjisinin

2.4 eV'tan ($x = 0$) 2.57 eV'a ($x = 1$) arttığını gösterdi. Ortaya çıkarılan bant enerji değerlerine göre bant boşluğu enerjisinin kompozisyona bağlılığını gösteren bir grafik çizildi.

Anahtar Kelimeler: GaSe, GaS, Elipsometri, Katmanlı kristaller, Yapısal özellikler





To My Supervisor and Co-Supervisor

ACKNOWLEDGMENTS

I would never have been able to finish my thesis without the guidance of my supervisor Assoc. Prof. Dr. Mehmet Işık and co-supervisor Assoc. Prof. Dr. Filiz Korkmaz Özkan. I would like to Express my deepest thank to them for their excellent guidance, caring and patientence.

TABLE OF CONTENTS

ABSTRACT	iii
ÖZ	iv
DEDICATION.....	v
ACKNOWLEDGMENTS	vi
TABLE OF CONTENTS	vii
LIST OF TABLES	ix
LIST OF FIGURES	xi
CHAPTER	
1. INTRODUCTION	1
1.1 GaSe crystal	2
1.2 GaS crystal	6
1.3 GaS _x Se _{1-x} mixed crystals	9
1.4 Present study.....	10
2. THEORETICAL APPROACH	11
2.1 Introduction	11
2.2 Band structure of Semiconductors.....	11
2.3 X-ray Diffraction.....	14
2.4 Energy Dispersive Spectroscopy	17
2.5 Fourier transform infrared spectroscopy.....	18

2.6 Ellipsometry.....	20
3. EXPERIMENTAL DETAILS.....	23
3.1 Energy Dispersive Spectroscopy	24
3.2 X-ray Diffraction.....	25
3.3 Fourier transform infrared spectroscopy.....	26
3.4 Ellipsometry	26
4. RESULTS AND DISCUSSION	28
4.1 Results of Energy Dispersive Spectroscopy Analyses.....	28
4.2 Results of X-ray Diffraction.....	31
4.1 Results of Fourier Transform Infrared Spectroscopy Measurements.....	36
4.1 Results of Ellipsometry Measurements.....	39
5. CONCLUSIONS	43
REFERENCES	45

LIST OF TABLES

TABLE

2.1 Characteristics of the seven crystals classes.....	16
4.1. EDSA results for GaS _x Se _{1-x} mixed crystals.....	31
4.2 Positions (2θ) of observed diffraction peaks in XRD patterns.....	34
4.3 The frequencies (cm^{-1}) reported previously by different methods and observed in infrared transmittance spectra.....	38
4.4 Band gap energy values (eV) of GaS _x Se _{1-x} mixed crystals and fitting parameters according to Eq. 4.1.....	41

LIST OF FIGURES

FIGURES

1.1 (a) Atomic configuration of GaSe. Open and dark circles present Se and Ga atoms, respectively. (b) Perspective and top views of a unit of GaSe	3
1.2 The electronic energy band structures of GaSe.....	4
1.3 Atomic structure of GaS. Yellow and red circles represent the S and Ga, respectively.....	7
1.4 The electronic energy band structures of GaSe.....	7
2.1 (a) Position dependency of potential energy of a conduction electron (b) Square well periodic potential suggested by Kronig Penney.....	12
2.2 The extended-zone representation k -vector and energy dependency.....	13
2.3 Simple diagram of reduced-zone representation.....	13
2.4 X-ray diffraction from a crystalline structure.....	15
2.5 Principles of energy dispersive spectroscopy.....	17
2.6 Possible vibrational modes of a triatomic molecule are stretching, bending and rocking.....	19
2.7 Reflection of p- and s- polarized light waves.....	20
3.1 Some of the crystals used for characterization.....	23
3.2 (a) Simple schematic representation of scanning electron microscope and (b) used SEM device.....	24
3.3 (a) Simple schematic representation of x-ray diffractometer microscope and (b) used SEM device.....	25
3.4 SOPRA GES-5E rotating polarizer ellipsometer.....	27
4.1 Energy dispersive spectra of $\text{GaS}_x\text{Se}_{1-x}$ mixed crystals.....	29
4.2 X-ray powder diffraction patterns of $\text{GaS}_x\text{Se}_{1-x}$ mixed crystals.....	33
4.3 Compositional dependence of lattice parameters.....	35

4.4 Infrared transmittance spectra of $\text{GaS}_x\text{Se}_{1-x}$ mixed crystals	36
4.5 $(\alpha h\nu)^{1/2}$ vs. $(h\nu)$ plots of $\text{GaS}_x\text{Se}_{1-x}$ mixed crystals.....	39
4.6 Compositional dependence of band gap energies (stars) and fitted line according to Eq. 4.1.....	42



CHAPTER I

INTRODUCTION

Semiconductors, normally being insulators, exhibit conductive properties under the external effects like heat, light, magnetic field or voltage. They turn into insulators when the applied external effects are removed. Due to this property, semiconductors have an important position in the production of electronic devices. Transistors, diodes, photovoltaic solar cells, detectors which are based on the semiconductor materials, are effective electronic devices in today's technology. Researches on the structural, optical and electrical characterization of semiconductor materials used in above-mentioned devices and/or similar ones contributes to the improvement of electronic device applications.

III, IV, V and VI group elements and the complexes formed by these elements are currently the most frequently used materials in semiconductor devices. Therefore, the manufacturing and analysis of these elements and their complexes contribute greatly to the semiconductor technology. Among various types, A^{III} B^{VI} type complexes are particularly important and attractive due to the structural, optical and electrical properties that they exhibit. GaSe, GaS and InSe are three important members of this group. These materials are especially used in solar cells, application of optoelectronic devices, transistors, nonlinear optical applications and in many other fields. These materials have their individual character; however, when two such complexes are combined ($\text{GaSe} + \text{InSe} = \text{Ga}_x\text{In}_{1-x}\text{Se}$ ve $\text{GaSe} + \text{GaS} = \text{GaS}_x\text{Se}_{1-x}$), the resulting ternary compound shows different properties, which are the combination of individual characters. Thus, this method introduces new materials that have the potential to be used in semiconductor technology.

In the present thesis, structural and ellipsometric properties of $\text{GaS}_x\text{Se}_{1-x}$ ($0 \leq x \leq 1$) will be investigated. GaSe and GaS semiconducting compounds form a series

of mixed crystals $\text{GaS}_x\text{Se}_{1-x}$ for x values between 0 and 1 without any restriction. Taking into account the attractive position of constituent semiconducting materials, GaSe and GaS, in technological applications, $\text{GaS}_x\text{Se}_{1-x}$ mixed crystals can be thought as potential candidates in the same and/or similar application areas. Moreover, possibility of growing mixed crystal in any desired ratio of GaSe and GaS presents a valuable advantage to researchers to grow a material having properties between those of constituent compounds. For example, by adjusting x value, a compound with a desired band gap, conductivity, mobility and so on can be grown. In the literature, there are many reports concerning the characterization of GaSe, GaS and $\text{GaS}_x\text{Se}_{1-x}$ mixed crystals. Firstly, it will be worthwhile to present literature knowledge on the main characteristic properties of GaSe and GaS. Then previous studies on the $\text{GaS}_x\text{Se}_{1-x}$ will be summarized.

1.1 GaSe crystal

GaSe, one of the members of III-VI type semiconducting group, has been investigated in both experimental and theoretical reports to understand its usability in the technological applications such solar cells, transistors, heterojunctions, second harmonic generator. This attractive compound has wide application areas due to its characteristic structural, optical and electrical properties.

GaSe layered semiconducting crystals are characterized by highly anisotropic bonding forces. This type of force is the results of the fact that bonding within the layers is rather stronger than bonding perpendicular to layers. The covalently bounded layers of GaSe crystal consist of four monatomic sheets in the order of Se-Ga-Ga-Se. A single layer is hexagonally ordered and c -axis is perpendicular to the layers. A simple presentation of atomic configuration of GaSe layered crystal is shown in Fig. 1.1. Crystal structure of GaSe have four modifications: ϵ , β , γ and δ [1]. Figure presents the most symmetric, β modification. The x-ray diffraction analyses resulted with lattice parameters of a and c of the hexagonal structure as 0.375 nm and 1.595 nm, respectively [2]. Theoretical studies on GaSe revealed the electronic energy band structures of GaSe. The results of density functional theory studies indicated the electronic band structure as presented in Fig. 1.2.

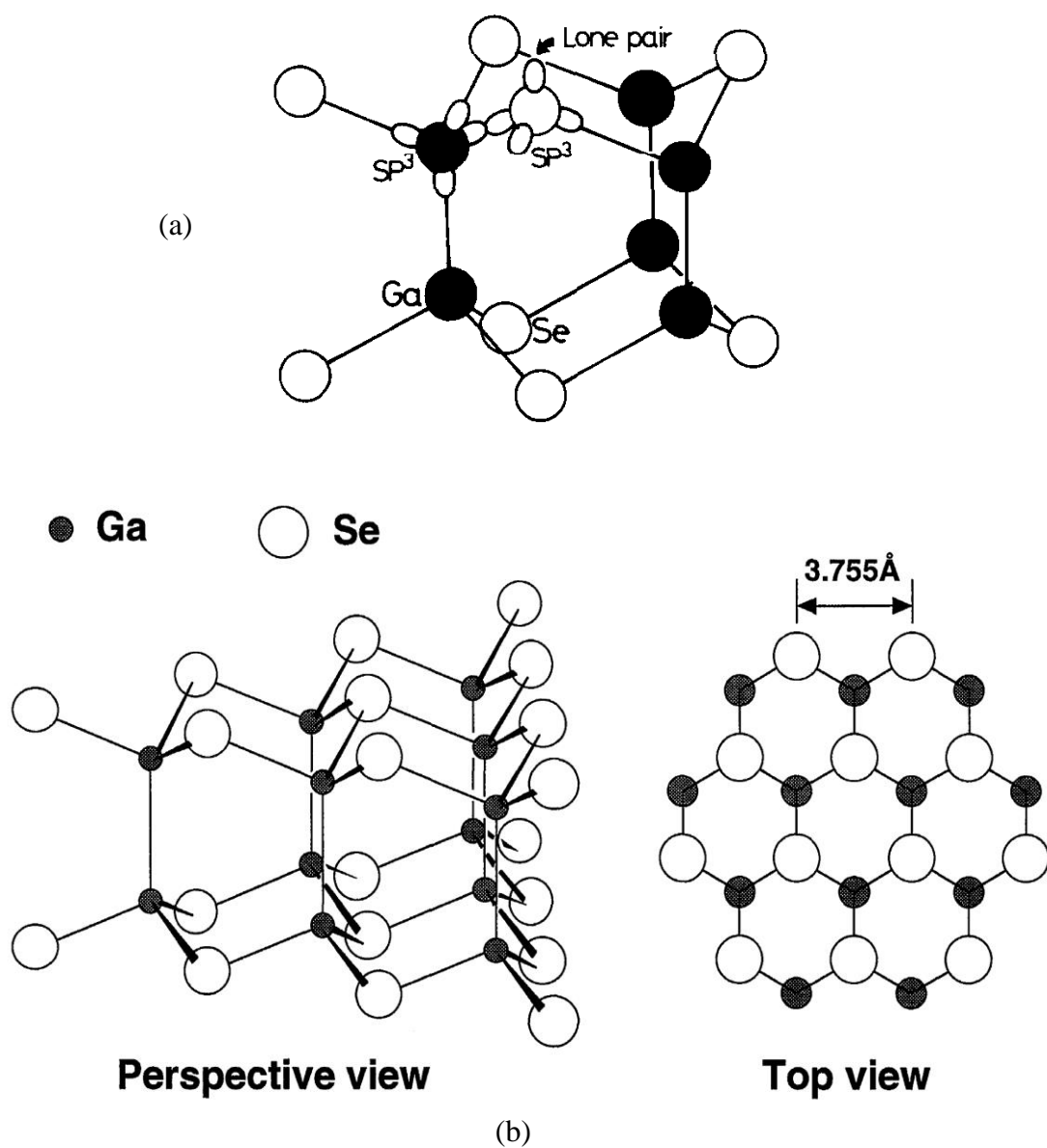


Figure 1.1. (a) Atomic configuration of GaSe. Open and dark circles present Se and Ga atoms, respectively [3]. (b) Perspective and top views of a unit of GaSe [4].

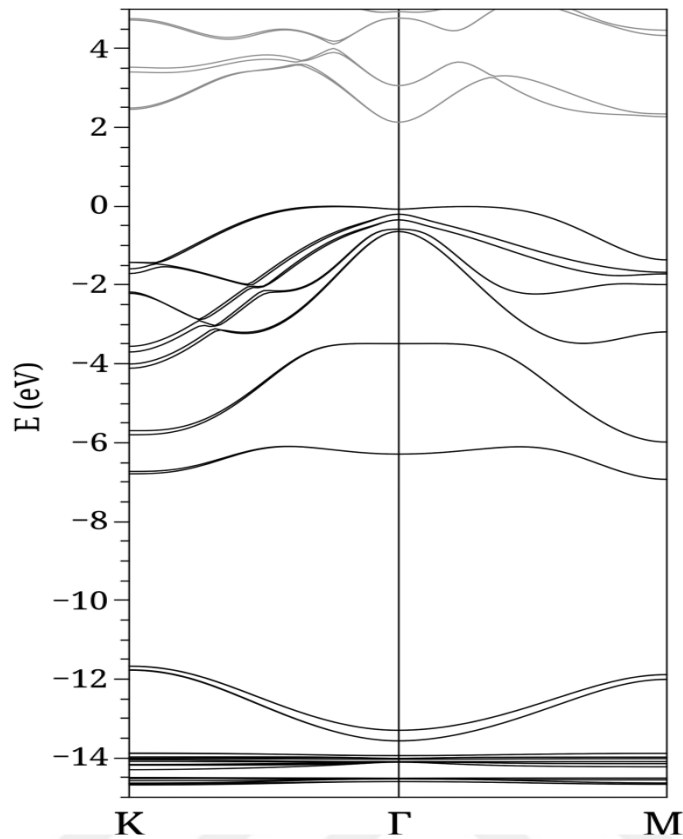


Figure 1.2. The electronic energy band structures of GaSe [5].

GaSe have band gap energy of around 2.0 eV which is very useful gap value for optoelectronic applications. There are different reports on band gap calculation of GaSe in literature. Karabulut et al. revealed the direct band gap energy of GaSe single crystal as 1.985 eV using the analyses of optical absorption spectra obtained at room temperature [6]. Aulich et al. found the indirect band gap energies of p-type semiconducting GaSe crystal at 77 and 4.2 K temperatures as 2.065 and 2.075 eV, respectively [7]. Analyses of piezoreflectance measurements showed that GaSe crystals have band gap energy of 1.988 eV at room temperature [8].

Optical properties of GaSe single crystals were also investigated using ellipsometry measurements. Spectral dependencies of optical parameters of dielectric function, refractive index and extinction coefficient were reported in Ref. [9]. Interband transition energies were found using second-energy-derivative spectra of

dielectric function. Seven critical points with energies of 3.23, 3.75, 4.03, 4.69, 5.02, 5.45 and 5.72 eV were found from the analyses.

Temperature dependent transmission and room temperature reflection measurements were carried out on GaSe single crystals in the temperature range of 10-280 K and wavelength range of 380-1100 nm [10]. Analyses of the absorption coefficient showed that indirect band gap energy of the crystal increases from 1.98 to 2.1 eV as temperature is decreased from 280 to 10 K. In the same paper, oscillator energy, dispersion energy, oscillator strength and zero frequency refractive index values were also reported using optical models proposed in literature.

Defect centers in undoped GaSe single crystals were revealed using thermally stimulated current (TSC) [11] and thermoluminescence (TL) [12] measurements. TSC spectra obtained in the temperature range of 10-300 K presented peaks around 86, 170 and 190 K. Curve fit analyses showed that these peaks come into existence due to presence of trapping centers at 0.02, 0.10 and 0.26 eV. Thermoluminescence experiments were performed in low temperature range of 30-300 K to get information about the shallow trapping centers. Thermoluminescence spectra exhibited peaks around 75, 142, 158 and 203 K. Results of curve fit and initial rise methods were in good agreement about the presence of trapping centers at 0.14, 0.18, 0.24 and 0.37 eV. In both paper, capture cross sections and attempt to escape frequencies of revealed centers were calculated.

Photoluminescence (PL) experiments were carried out on GaSe single crystals in the temperature range of 10-300 K [13]. PL spectra presented two wide bands. Temperature dependency of emission intensities were analyzed and two shallow acceptor levels at 14 and 76 meV were revealed. Using these shallow energy values and emission energy, authors concluded that there are two deep donor centers at 163 and 264 meV. In another paper on PL studies of GaSe crystal reported by another research group, authors observed two peaks in PL spectra with energies of 2.086 and 2.067 eV [14]. Temperature dependency of PL spectra showed that crystal has band gap energy of 2.112 eV.

It will be worthwhile to give also brief information about the technological applications of GaSe material. In literature there are many papers concerning the usage of GaSe in different applications. These papers showed that GaSe has potential

to be used as p-GaSe/n-InSe heterojunction [15], modulator for He-Ne laser [16], nonlinear optical material [17], second harmonic generator [18], ultrathin layer transistor [19], detector [20].

1.2 GaS crystal

GaS is another important member of III-VI semiconductors. The crystal structure of GaS shows similarity to that of GaSe. GaS consists of covalently bonded stacks of four atomic layers. The stacking sequence of S-Ga-Ga-S is held together by weak van der Waals interactions [21]. Depending on how the quadruple layers stack on top of each other, there are typically three different crystal structures: β , ϵ and γ . The atomic structure of β modification of GaS is presented in Fig. 1.3 [5]. The polytypes can be identified using Raman or infrared spectroscopy. The bulk GaS crystallizes in the β phase with space group no. 194, $D_{6h}^4(P6_3/mmc)$ [22]. It crystallizes in the hexagonal structure with lattice parameters of (JCPDS card, No. 30-0576): $a = 0.359$ and $c = 1.549$ nm [23]. The bond distances of the hexagonal layered GaS structure for the Ga–Ga and Ga–S are 0.248 and 0.237 nm, respectively. Accordingly, the thickness of one formula unit is approximately 0.76 nm [23]. The electronic energy band structures of GaS were revealed from theoretical study using density functional theory. Fig. 1.4 shows the reported electronic band structure of the crystal [5].

Since GaS has broad range of potential technological applications, structural, optical and electrical characterization of GaS takes very important role for researchers working in relevant areas. Analyses of data taken from optical absorption experiments on GaS single crystals at room temperature resulted in both indirect and direct band gap energies of 2.59 and 3.04 eV, respectively [24]. These optical band gap energies make the crystal a promising material in the fabrication of near-blue-light emitting devices.

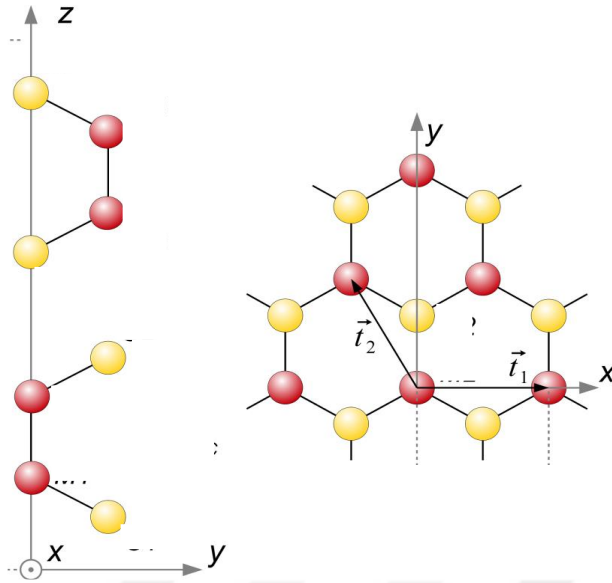


Figure 1.3. Atomic structure of GaS. Yellow and red circles represent the S and Ga, respectively [5].

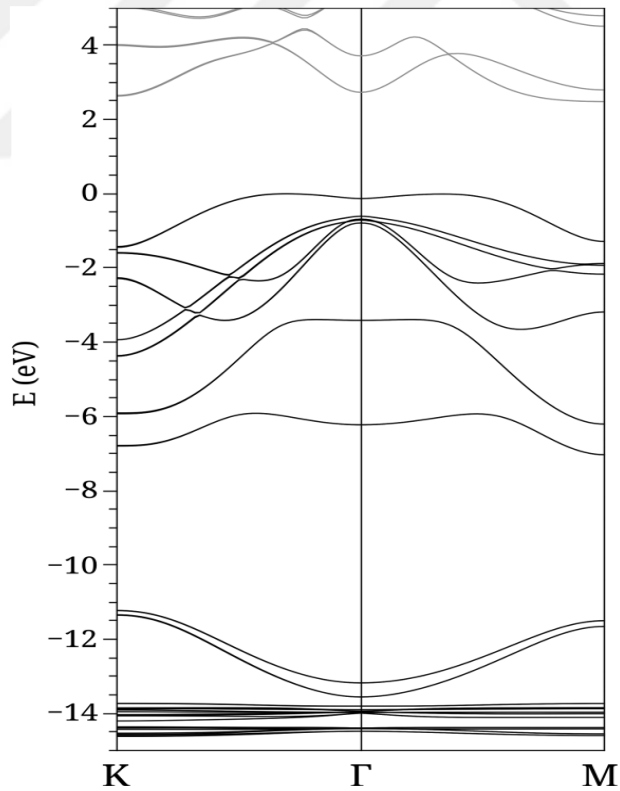


Figure 1.4. The electronic energy band structures of GaS [5].

Temperature dependent absorption and piezorefectance measurements were accomplished to investigate the optical properties of GaS [25]. The analyses of the experiments performed in the 13-300 K temperature range pointed out the presence of indirect band gap energy of 2.53 eV. Average phonon energy of the crystal was also reported as 26 meV.

Temperature dependent transmission and room temperature reflection experiments were accomplished to get variation of band gap energy with temperature [26]. Derivative analyses of the absorption coefficient indicated the coexistence of indirect and direct transitions in the crystal at room temperature with energies of 2.53 and 2.63 eV, respectively. Temperature dependent investigations showed that indirect and direct band gap energies increases by 0.09 and 0.15 eV, respectively, when the temperature is decreased to 10 K. Oscillator energy, dispersion energy, oscillator strength and zero frequency refractive index values were also reported using Wemple-DiDomenico single effective oscillator model.

Spectroscopic ellipsometry measurements were carried out in the 1.2-6.2 eV range [27]. Optical constants; refractive index, extinction coefficient, real and imaginary parts of dielectric function were obtained using simple sample-ambient optical model. Second derivative of real and imaginary components of dielectric function were plotted and analyzed to get the critical points. Five interband transitions were found with energies of 3.95, 4.22, 4.51, 4.75 and 5.50 eV.

Photoluminescence experiments were carried out on GaS single crystals at different temperatures and different excitation intensities [28]. PL spectra observed at 10 K presented three broad peaks centered at 2.22, 2.02 and 1.59 eV. Analyses of temperature dependent experimental data showed that there exist two donor levels at 13 and 17 meV. Authors also proposed a simple band model showing transitions responsible for PL emissions.

Defects in undoped GaS single crystals were investigated using thermally stimulated current and thermoluminescence measurement in the below room temperature region. Thermally stimulated current measurements performed in the 10-300 K range and at a heating rate of 0.10 K/s presented four peaks [29]. Analyses of the glow curve revealed that TSC spectra is composed of six individual peaks. Activation energies of these six trapping centers were found as 0.05, 0.06, 0.12, 0.63,

0.71 and 0.75 eV. Capture cross sections and attempt to escape frequencies of these centers were also reported. Thermoluminescence experiments were used to obtain information about the shallow trapping centers in the crystal. Delice et al. reported the presence of three centers at 52, 200 and 304 meV as a result of observed TL glow curve in the temperature range of 10-230 K [30].

1.3 GaS_xSe_{1-x} mixed crystals

GaS_xSe_{1-x} mixed crystals grown by Bridgman method were optically characterized by transmission and piezoreflectance measurements in the composition range of $0 \leq x \leq 0.5$ [31]. The compositional dependence of band gap energy were plotted and increase of gap energy from 1.986 eV (GaSe) to 2.370 eV (GaS_{0.5}Se_{0.5}) was determined.

Compositional dependence of lattice parameters and higher interband transition energies were determined for GaS_xSe_{1-x} mixed crystals for compositional range of $0 \leq x \leq 1.0$ [32]. In the x-ray diffraction pattern, shift of the diffraction peaks to higher angles were detected as sulfur composition is increased in the mixed crystals. Piezoreflectance spectra obtained at 15 and 300 K indicated the presence of five transition features having energies between 1.988 and 4.439 eV.

Spectral dependencies of real and imaginary components of dielectric function, refractive index and extinction coefficient of GaS_xSe_{1-x} mixed crystals ($0 \leq x \leq 1$) were determined from ellipsometry measurements [33]. Critical point energies were revealed from the second derivative of components of dielectric function. The variation of critical point energies with composition was plotted and these energies were related to each other by taking into consideration the change of band gap energy with composition.

Optical properties of GaS_xSe_{1-x} mixed crystals ($0 \leq x \leq 1$) were also investigated from transmission and reflection measurements [34]. Derivative spectra of transmittance and reflectance were used to find the band gap energies of the studied crystals. The increase of gap energy from 1.99 eV (GaSe) to 2.55 eV (GaS) quadratically was reported in this reference. Spectral dependencies of refractive indices of the used samples were also presented and it was shown that refractive index increases with decreasing gap energy for mixed crystals.

In addition to above given references, there are many papers on the characterization of single crystals for a specific composition of x . Structural, optical and electrical properties of crystals were investigated by many research groups by performing different experimental techniques such photoluminescence, raman measurements, Hall effect measurements, thermally stimulated current, thermoluminescence.

1.4 Present Study

In the present thesis, $\text{GaS}_x\text{Se}_{1-x}$ mixed crystals are characterized structurally and optically using experimental techniques of x-ray diffraction, energy dispersive spectroscopy, fourier transform infrared spectroscopy and ellipsometry. Some of these techniques were previously applied on some members of $\text{GaS}_x\text{Se}_{1-x}$ mixed crystals. However, in the present thesis, a detailed analyses and discussions which are not presented in literature are given. Compositional dependence of obtained results is investigated and effect of increase of sulfur or selenium composition in the mixed crystals is discussed. In the thesis, a theoretical information about the applied techniques is given in chapter 2. Experimental details such devices, measurement parameters are mentioned in chapter 3. The results of used techniques and discussion about the results are detailed in chapter 4. In the last chapter 5, physical interpretations and a short summary of results are presented.

CHAPTER II

THEORETICAL APPROACH

2.1 Introduction

Semiconductors are materials having band gap energy and electrical resistivity values between those of metals and insulators. The resistivity and band gap energy ranges for semiconductors are 10^{-3} - 10^{+9} Ωcm and 2-3 eV, respectively. The most important property of semiconductors giving these materials potential to be used in technological applications is that electrical conductivities of semiconductors can be controlled by applying some external effects such temperature and doping. There are many technological devices designed using semiconductor materials. Transistors, solar cells, diodes and detectors are some of these devices. When the literature is searched carefully, it is noticed that there are lots of papers on the characterization of binary, ternary and quaternary semiconductor compounds. The structural, optical and electrical characterization of semiconductors grown using different type of elements present attractive information to researchers working on technological applications of these compounds. For that reason, each semiconductor material must be investigated using possible all experimental techniques. Present thesis aims to investigate the $\text{GaS}_x\text{Se}_{1-x}$ semiconductor crystals using structural and optical characterization methods. In the present chapter, information about the theoretical background of the used experimental techniques are given.

2.2 Band Structure of Semiconductors

Atoms in the crystalline structures are periodically ordered in three dimensions. When Schrödinger equation is used to study the state of an electron

inside this ordered structure, it is applied by considering that electrons are inside a periodic potential of $V(r) = V(r + a)$. The state of an electron inside this periodic structure is defined as

$$\psi(r) = u(r) \exp(ikr). \quad (2.1)$$

In this equation $u(r)$ is called as Bloch function and periodic as $u(r) = u(r + a)$. In Eq 2.1, k and r symbolize the wave vector and position vector, respectively. There is a need for some simplifications to study the state of an electron inside this periodic potential. Kronig Penney model simplifies this periodic potential and this model is one of the basics of solid state physics [35]. Fig. 2.1a shows the positional dependence of potential energy of an electron while Fig. 2.1b presents the approximation model proposed by Kronig Penney.

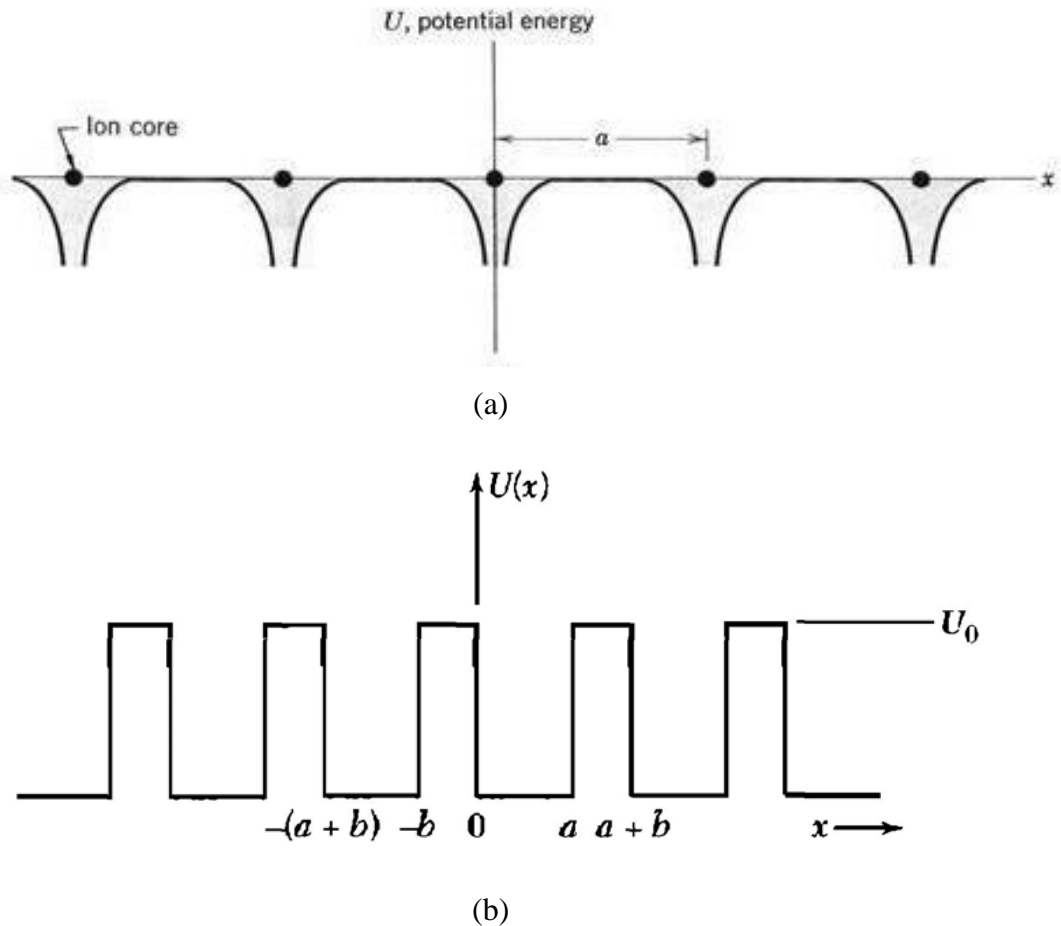


Figure 2.1. (a) Position dependency of potential energy of a conduction electron (b) Square well periodic potential suggested by Kronig Penney [36]

When the wave equation of an electron under periodic potential is solved, there exist some important results. The most important one of these results for semiconductor technology is that there exist energy band gaps allowed to be occupied by semiconductors. Fig. 2.2 is the extended zone representation which shows the dependency of energy on k -vector. Fig. 2.3 is a simple diagram of reduced zone representation.

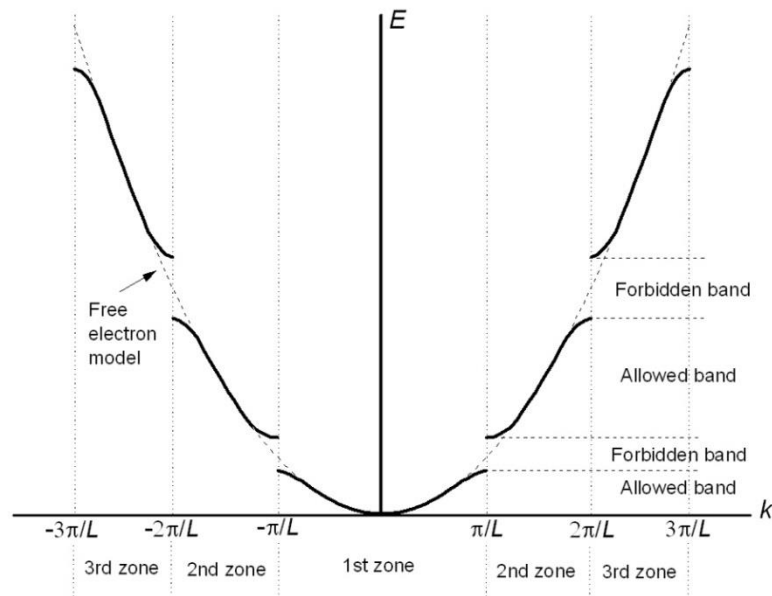


Figure 2.2. The extended-zone representation k -vector and energy dependency [37].

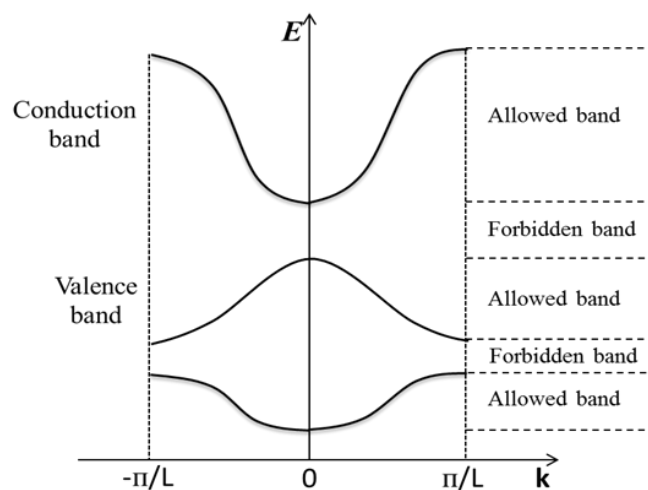


Figure 2.3. Simple diagram of reduced-zone representation [37].

In the band structures of semiconductors, there is an energy value called as energy gap or band gap energy which is very important value for semiconductor technology. The highest energy band occupied by electrons at absolute zero temperature is called as valence band and the lowest energy band above this valence band is called as conduction band. The energy difference between these two bands is called as band gap energy. Metals, semiconductors and insulators differ according to bigness of this energy band gap value. In the metals, there is no gap between conduction and valence bands. These bands are overlapped in metals. Electrons can excite to conduction band by getting very small energy and take role in conductivity of the materials. In the insulators, this gap is very high and generally bigger than 3-4 eV. The materials having gap energy between those of metals and insulators are called as semiconductors. At absolute zero temperature, all electrons are found in valence band. Electrons can have probability to be excited to conduction band at high temperatures. Electrons excited to conduction band contribute to electrical conduction.

2.3 X-ray Diffraction

Atoms are periodically arranged in the crystal structure. X-ray diffraction is one of the most important experimental techniques used to get information about the structural properties of crystals. The interatomic distance in the crystal is very small than the wavelength of visible light. For that reason, light waves reflecting from the parallel planes inside crystal structure is not used for characterization purpose. X-rays have wavelengths (0.15-0.40 nm) in the same order with distance between parallel planes of atomic structure. This small wavelength property provides x-rays possibility to be used in structural characterizations using diffraction effect.

Fig. 2.4 shows a small part of parallel lattice planes having distance of d between them. When the x-rays are fallen on a screen after reflecting from the planes, dark and bright regions are observed on the screen. The mathematical relation to get constructive interference is given as

$$2d_{hkl} \sin \theta = n\lambda \quad n = 0, 1, 2, 3, \dots \quad (2.2)$$

This equation tells us that when the path difference ($2d\sin\theta$) is equal to integer (n) multiple of wavelength (λ), constructive interference is formed by the reflected x-rays. This law called as Bragg law is formulated by famous scientist W.L. Bragg [38]. Bragg law is a result of periodicity of crystal structure. In the XRD experiments, plot of incident angle (2θ) vs. intensity of reflected light is obtained. When this data was analyzed, interplanar spacing (d), lattice parameters (a , b and c), Miller indices (h , k and l) and angles (α , β ve γ) are found. There are seven different crystal system in the solids. Table 2.1 presents the properties of these systems.

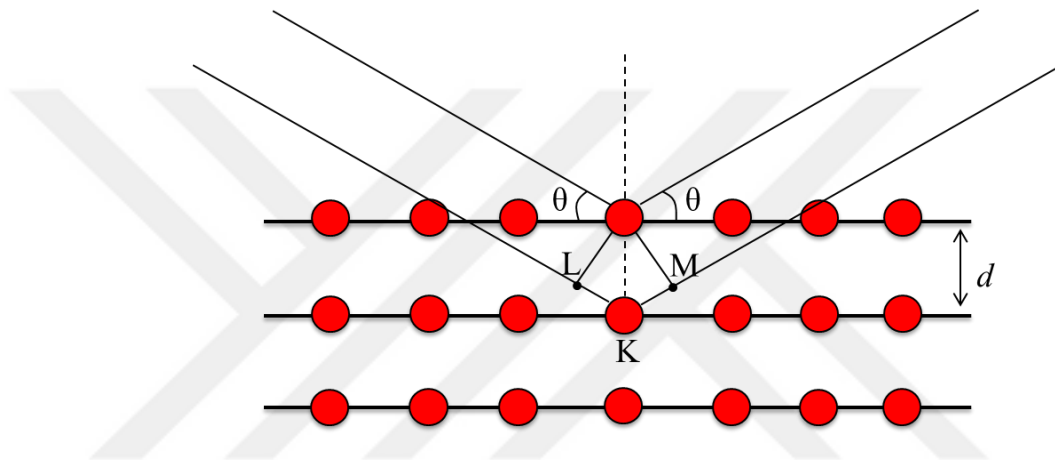


Figure 2.4. X-ray diffraction from a crystalline structure

Table 2.1. Characteristics of the seven crystal classes.

Crystal System	a : b : c	Axial Angles	$\frac{1}{d_{hkl}^2}$
Cubic	1 : 1 : 1	$\alpha = \beta = \gamma = 90^\circ$	$\frac{h^2 + k^2 + l^2}{a^2}$
Tetragonal	1 : 1 : c	$\alpha = \beta = \gamma = 90^\circ$	$\frac{h^2 + k^2}{a^2} + \frac{l^2}{c^2}$
Orthorhombic	a : 1 : c	$\alpha = \beta = \gamma = 90^\circ$	$\frac{h^2}{a^2} + \frac{k^2}{b^2} + \frac{l^2}{c^2}$
Hexagonal	1 : 1 : c	$\alpha = \beta = 90^\circ$ $\gamma = 120^\circ$	$\frac{4}{3} \frac{h^2 + hk + k^2}{a^2} + \frac{l^2}{c^2}$
Rhombo-hedral	1 : 1 : 1	$\alpha = \beta = \gamma \neq 90^\circ$	$\frac{(h^2 + k^2 + l^2) \sin^2 \alpha + 2(hk + hl + kl)(\cos^2 \alpha - \cos \alpha)}{a^2(1 - 3 \cos^2 \alpha + 2 \cos^3 \alpha)}$
Monoclinic	a : 1 : c	$\alpha = \gamma = 90^\circ$ $\beta \neq 90^\circ$	$\frac{h^2}{a^2 \sin^2 \beta} + \frac{k^2}{b^2} + \frac{l^2}{c^2 \sin^2 \beta} - \frac{2hl \cos \beta}{ac \sin^2 \beta}$
Triclinic	a : 1 : c	$\alpha \neq \beta \neq \gamma \neq 90^\circ$	$\frac{1}{\left[1 + 2 \cos(\alpha) \cos(\beta) \cos(\gamma) - \cos^2(\alpha) - \cos^2(\beta) - \cos^2(\gamma) \right]}$ $\times \left[\frac{h^2 \sin^2(\alpha)}{a^2} + \frac{k^2 \sin^2(\beta)}{b^2} + \frac{l^2 \sin^2(\gamma)}{c^2} \right]$ $+ \frac{2hk}{ab} (\cos(\alpha) \cos(\beta) - \cos(\gamma)) + \frac{2kl}{bc} (\cos(\beta) \cos(\gamma) - \cos(\alpha)) + \frac{2lh}{ac} (\cos(\gamma) \cos(\alpha) - \cos(\beta))$

2.4 Energy Dispersive Spectroscopy

Energy dispersive spectroscopy (EDS) measurements is one of the most effective techniques used to get information about the compositions of elements in a solid material. This method is based on the analyses of emitted light existing as a result of interaction between the sample and x-rays. The basic physical background of EDS method is like that: Electrons are found in different energy shells being around nucleus. Fig. 2.5 shows a nucleus and K, L and M energy shells around this nucleus. L and M shells are divided into 3 and 5 subshells, respectively.

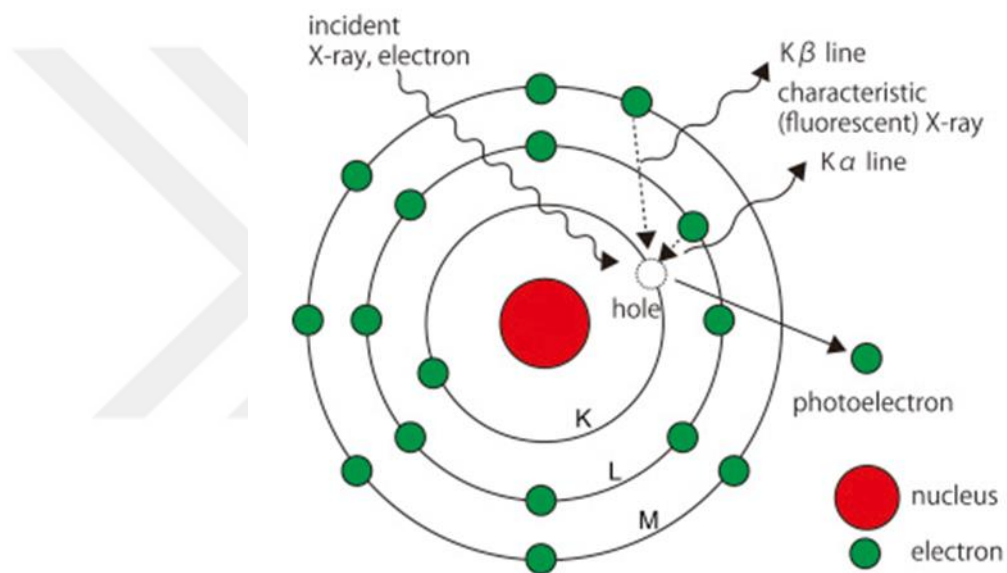


Figure 2.5 Principles of energy dispersive spectroscopy [39]

Since each element has characteristic atomic structure, the energy values between these mentioned shells differ from sample to sample. That means these energy values are like a fingerprint for elements. If an element is subjected to high energy, electrons in the inner shells leave the atoms by creating a hole in their left positions. Another electron in higher energy shell make transition to this hole and radiation having energy between the shells taking role in this transition is emitted. This is emitted radiation is in the form of x-rays and a value proportional to number of

emitted x-rays and their energies are obtained as a result of EDS experiments. Since energies of these emitted x-rays are characteristic property of used samples, EDS method is used to get compositions of elements within the material.

2.5 Fourier transform infrared spectroscopy

Infrared (IR) spectroscopy, which works through penetrating the vibrations of the molecules, examines the interaction between the electromagnetic radiationradioactivity in infrared region with the molecules' electric dipole moment. Moreover, it is a non-destructive method that provides immediate data on bond order, electrostatic interactions, H-bonding, charge distribution, protonation state, dynamics and kinetics of active molecular groups.

The radiation is absorbed and the gained energy excites the molecules which has the same vibrational energy levels, if the emitted radiation frequency is the same as the oscillation frequency of the molecule's vibration. Therefore, there are mainly three regions, which can be studied by IR spectroscopy, which ranges between 0.7 to 500 μm (20 to 1400 cm^{-1}) divided into three main ranges:

Near-IR: 0.8 to 2.5 μm or 4000 to 12500 cm^{-1}

Mid-IR: 2.5 to 25 μm or 400 to 4000 cm^{-1}

Far-IR: 25 to 100 μm or 10 to 400 cm^{-1}

An infrared spectrum is the plot of radiation absorption as a function of frequency (ν) or wavelength (λ), where $\nu = c / \lambda$ and $\lambda = c / \nu$; where c is the speed of light. The phenomenon of molecular vibration excitement of any sample provides unique absorption bands very closely to their position in every biological material that have the same groups of structures, which creates a frequency for each group. Thus, absorption spectra of the compounds are known by their functional group frequencies of their molecules, which are interactive to any surrounding, in structure, within molecule changes. Moreover, those frequencies are also known by due to the motion of the nuclei, which are such as; twisting, bending, rotating rocking and stretching modes (asymmetric and symmetric). Some of the vibrational

modes of a triatomic molecules are illustrated in Figure 2.6 below. Frequency values belonging to a specific mode of vibration are presented as (ν_s) for symmetric stretching, (ν_{as}) as for asymmetric stretching as (δ_s) for bending modes.

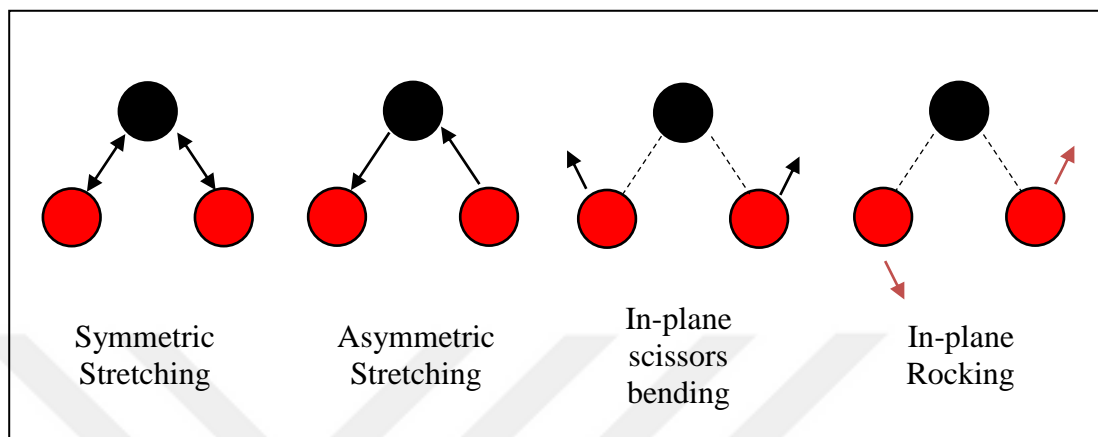


Figure 2.6 Possible vibrational modes of a triatomic molecule are stretching, bending and rocking.

There are two categories of vibration modes; stretching and bending. Bending modes has four types. In addition to the given two modes on the right of the Figure 2.6, there are out-of-plane wagging and twisting modes.

The infrared absorbance of a sample is calculated by using Beer-Lambert equation :

$$A = \log (I_0(\nu)) / (I(\nu)) \quad (2.3)$$

where $I_0(\nu)$ and $I(\nu)$ are the single beam spectra of the background and the sample, respectively.

2.5 Ellipsometry

Ellipsometry is one of the effective optical characterization techniques. This method is experimentally simple and nondestructive. Ellipsometry method uses the change of incident polarized light after reflected from the crystal surface. Ellipsometry name comes due to the shape of the reflected light which is commonly elliptical. In this method, two measurement data symbolized as ψ and Δ are given by ellipsometer. ψ and Δ indicate the amplitude ratio and phase shift of the parallel and perpendicular components of the reflected light. Fig. 2.7 shows reflection of a light wave from a sample surface. p - and s -polarization refers to the parallel and perpendicular position of incident and reflected light with respect to normal axis. Plane of incidence presented in the figure is called as the plane which electric fields of incident and reflected waves lie.

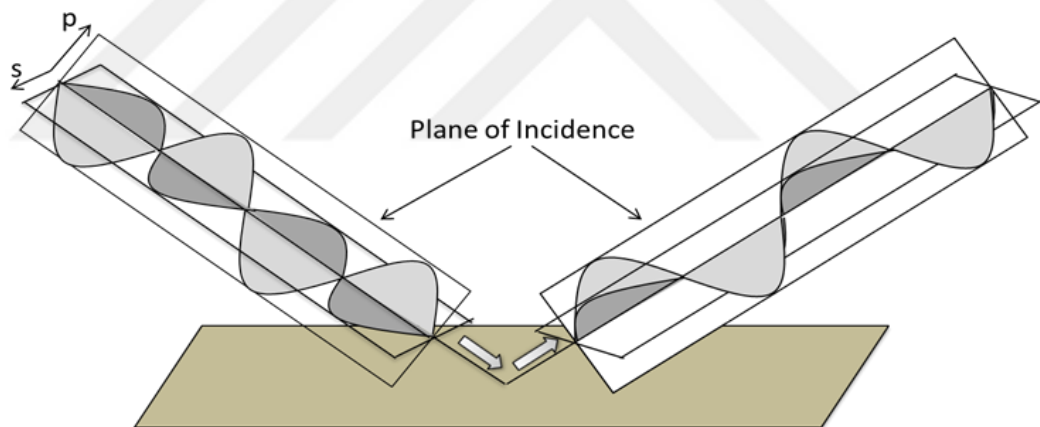


Figure 2.7 Reflection of p - and s - polarized light waves [40].

In the ellipsometry experiments, p - and s -polarized light waves are emitted onto sample surface. The amplitude and phase of the incident polarized light change after reflected from the surface. Experimental data, ψ and Δ , symbolize the amplitude ratio and phase difference between p and s polarizations. Theoretical

background of ellipsometry is based on Fresnel equations. ψ and Δ are related to amplitude reflection (r_p) and transmission (t_p) by the expressions [40]

$$\rho \equiv \tan(\psi) \exp(i\Delta) \equiv \frac{r_p}{r_s} \quad \text{for reflection measurements} \quad (2.4)$$

$$\rho \equiv \tan(\psi) \exp(i\Delta) \equiv \frac{t_p}{t_s} \quad \text{for transmission measurements.} \quad (2.5)$$

The analyses of ψ and Δ using different optical models which are based on the used sample gives opportunity to obtain optical parameters. If a bulk crystal is used, air/sample optical model formulated as [40]

$$\langle \varepsilon \rangle = \varepsilon = \sin^2 \theta_i \left[1 + \tan^2 \theta_i \left(\frac{1 - \rho}{1 + \rho} \right)^2 \right] . \quad (2.6)$$

is used to obtain the dielectric function (ε). θ_i corresponds to incident angle. Complex dielectric constant can be written in terms of its real (ε_1) and imaginary (ε_2) components as

$$\varepsilon = \varepsilon_1 + i\varepsilon_2 . \quad (2.7)$$

Air/sample optical model lets us to calculate the components of dielectric function. Then refractive index (n) and extinction coefficient (k) can be obtained using relations [41]

$$n = \left[\left(\varepsilon_1 + (\varepsilon_1^2 + \varepsilon_2^2)^{1/2} \right) / 2 \right]^{1/2} , \quad (2.8)$$

$$k = \left[\left(-\varepsilon_1 + (\varepsilon_1^2 + \varepsilon_2^2)^{1/2} \right) / 2 \right]^{1/2} . \quad (2.9)$$

When light beam is fallen onto a sample surface, some amount of this light is absorbed by sample. Absorption coefficient (α) is an optical parameter describing what distance would be covered by light beam throughout the sample before it is completely absorbed. This coefficient is related to extinction coefficient and wavelength (λ) of the light by the expression

$$\alpha = \frac{4\pi k}{\lambda} . \quad (2.10)$$

One of the most effective role of photon energy dependence of absorption coefficient is that it lets us to obtain band gap energy (E_g) of the used sample. Photon energy ($h\nu$) is related to absorption coefficient by [42]

$$(\alpha h\nu) = A(h\nu - E_g)^p , \quad (2.11)$$

where A is constant based on transition probability and p is an index which is equal to 2 and 1/2 for indirect and direct transitions, respectively.



CHAPTER III

EXPERIMENTAL DETAILS

$\text{GaS}_x\text{Se}_{1-x}$ mixed crystals were characterized structurally and optically using experimental techniques of energy dispersive spectroscopy (EDS), x-ray diffraction (XRD), Fourier-transform infrared (FTIR) spectroscopy and ellipsometry. $\text{GaS}_x\text{Se}_{1-x}$ mixed crystals were grown by Bridgman method. Fig. 3.1 shows a few samples of used mixed crystals. As can be seen when the sulfur concentration is increased in the compound, the color of the crystal gets lighter.

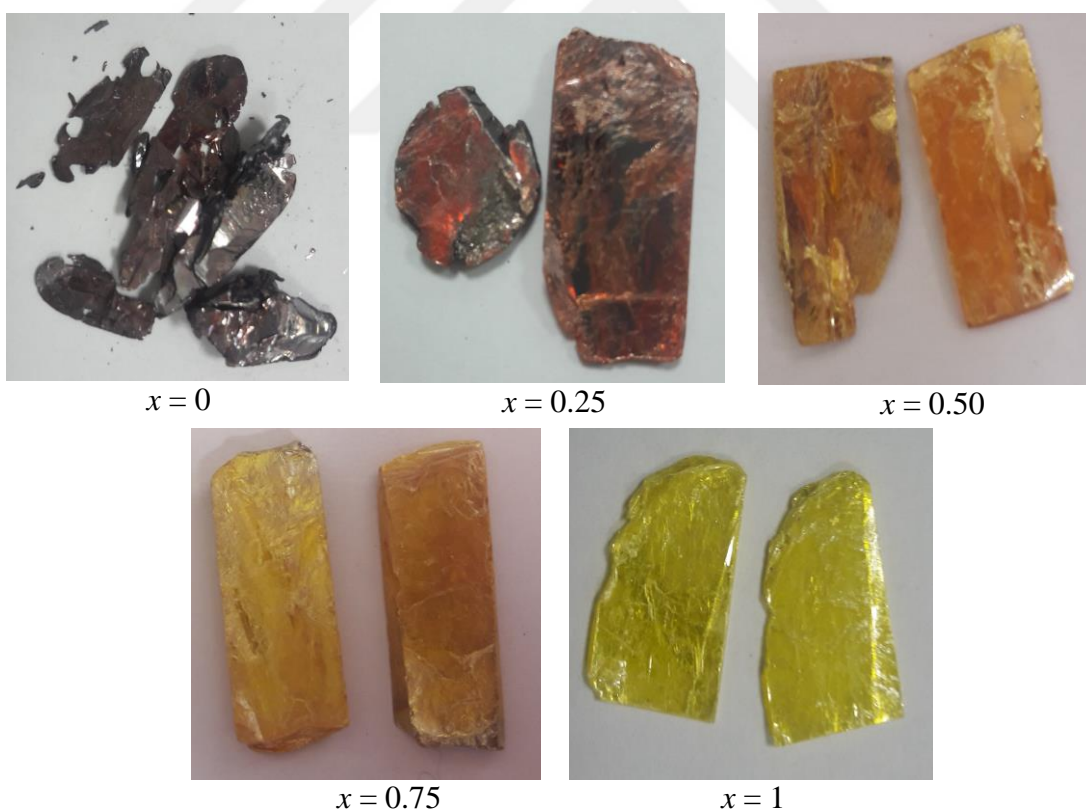


Figure 3.1 Some of the crystals used for characterization.

3.1 Energy Dispersive Spectroscopy

Chemical composition of elements in the grown crystals were determined using energy dispersive spectroscopy experiments. JSM-6400 scanning electron microscope (SEM) was used to carry out the measurements. SEM device has two equipments named as “Noran System6 X-ray microanalysis system” and “Semafore Digitizer”. After performing the measurements, device also make necessary analyses and give the compositional ratio of the used elements as output. Fig. 3.2 shows the simple schematic representation of and used SEM device.

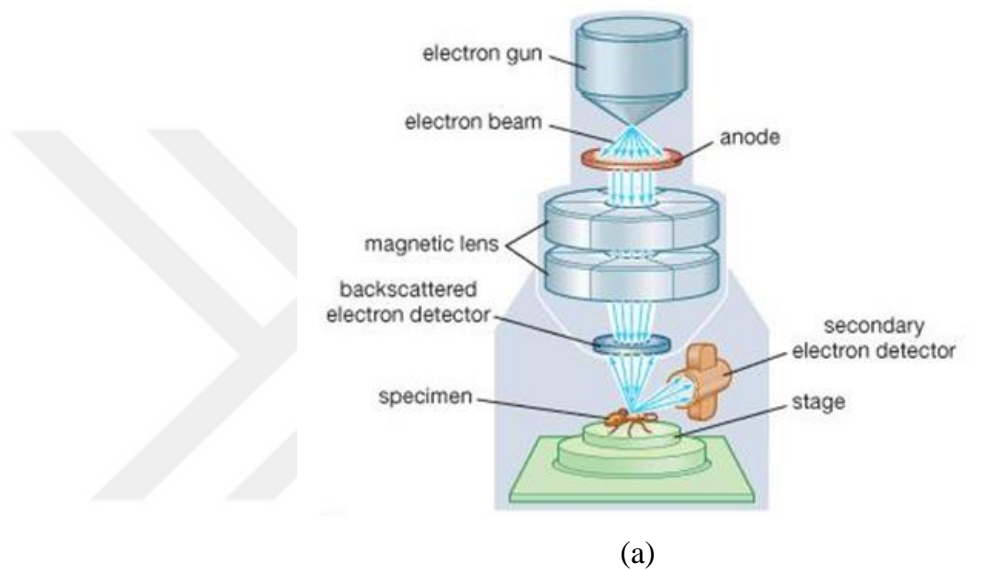
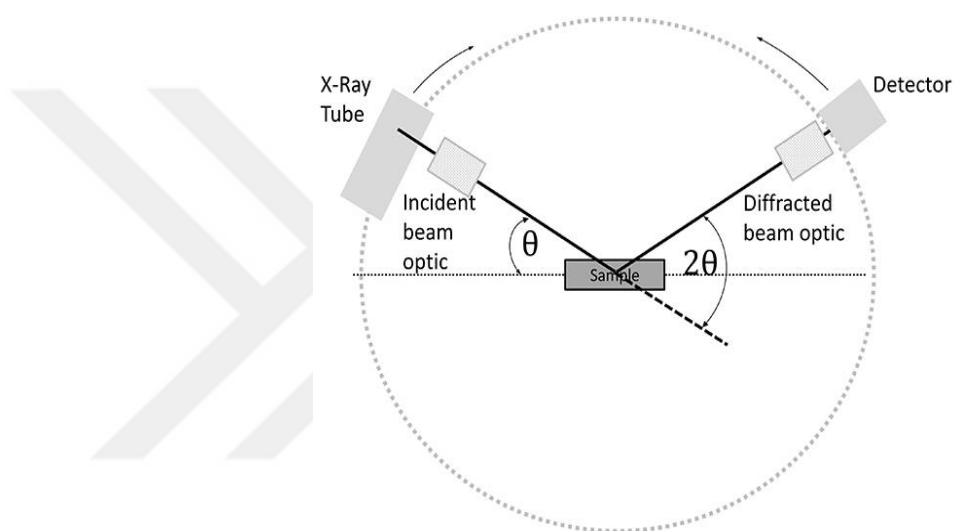


Figure 3.2. (a) Simple schematic representation of scanning electron microscope [43] and (b) used SEM device

3.2 X-ray Diffraction

X-ray diffraction experiments were accomplished to get information about the crystal structure of $\text{GaS}_x\text{Se}_{1-x}$ mixed crystals. “Rigaku miniflex” diffractometer working with $\text{CuK}\alpha$ radiation ($\lambda = 0.154049 \text{ nm}$) were used for measurements. The powder forms of each single crystal were placed into diffractometer and measurements were done in the diffraction angle range of $10\text{-}90^\circ$. Fig. 3.3 shows the schematic representation of the measurement set-up and used device for experiments. The crystalline parameters were obtained by analyzing the experimental data using TREOR90 software program.



(a)



(b)

Figure 3.3. (a) Simple schematic representation of x-ray diffractometer microscope [44] and (b) used device

3.3 Fourier transform infrared spectroscopy

FTIR is a nonperturbing spectroscopic tool that requires a small amount of sample. The instrument working principle relies on the classical principle of Michelson Interferometer. It involves a Globar source (a silicon carbide rod heated to about 1000 K), a beam splitter, two mirrors and a DTGS detector working at room temperature. The infrared measurements were performed with a Nicolet 6700 (Thermo Fisher Science Inc., USA) spectrometer. Atmospheric water vapour and carbon dioxide absorptions were subtracted from the sample spectra automatically. It is achieved by collecting a background spectrum (empty chamber measurement) before the sample measurement. After sample measurement is completed, the subtraction is automatically done by the spectrometer software OMNIC 8.2 (Thermo Fisher Scientific Inc.). Crystal samples were attached to a sample holder that stands vertical in front of the infrared beam. For each measurement, 16 scans were collected and averaged for 4 cm^{-1} final resolution. Scanning the sample multiple times increases the signal-to-noise ratio (S/N). Spectra were recorded without any digital enhancement methods.

Each crystal was measured at different positions and orientations. The best spectrum with minimum noise was chosen for the analysis. Spectra were shown as a plot of frequency versus transmittance.

3.4 Ellipsometry

Ellipsometry experiments were carried out on $\text{GaS}_x\text{Se}_{1-x}$ mixed crystals to investigate their optical properties. Air/sample optical model was used as analysis method to find extinction coefficient from ellipsometric parameters of ψ and Δ taken from software of ellipsometry device. SOPRA GES-5E rotating polarizer shown in Fig. 3.4 were used for measurements applied at room temperature and in the spectral range of 1.2-6.0 eV. The incident angle in the experiments were chosen as 70° . The thicknesses of the used mixed crystals were about 1 mm which is necessarily enough for application of air/sample optical model. The surfaces of the crystals were prepared to make them rough for experiments before measurements.



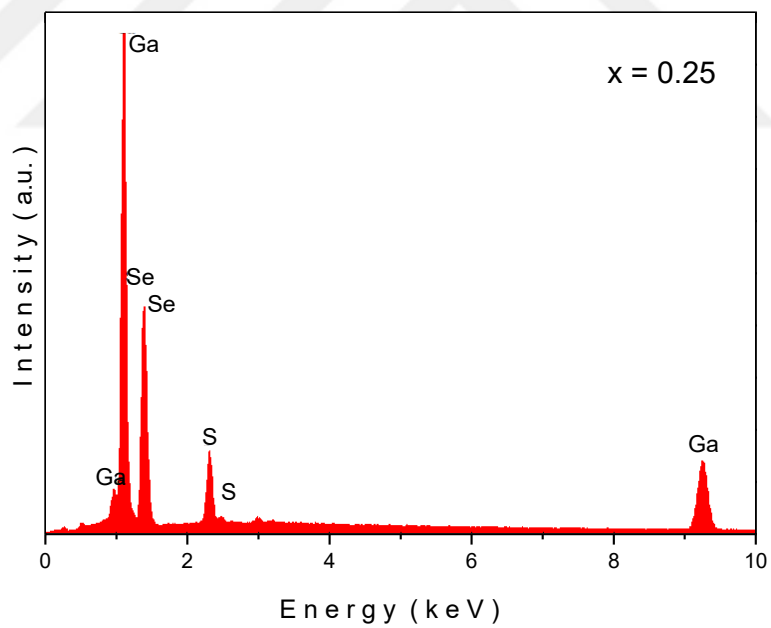
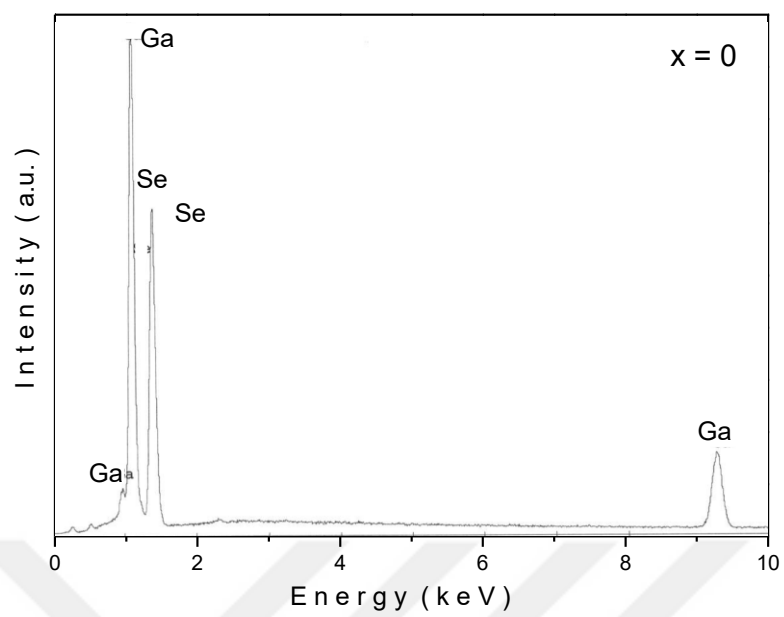
Figure 3.4 SOPRA GES-5E rotating polarizer ellipsometer.

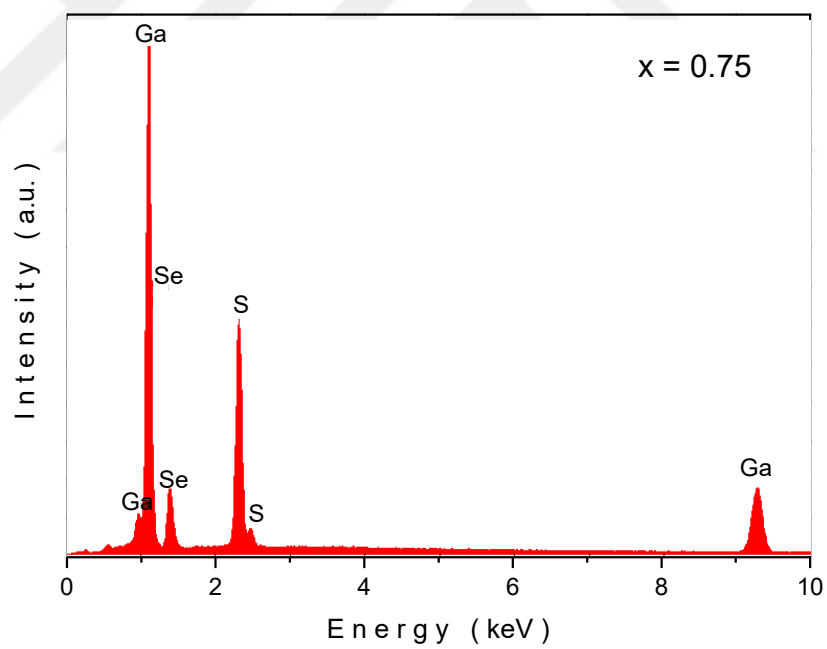
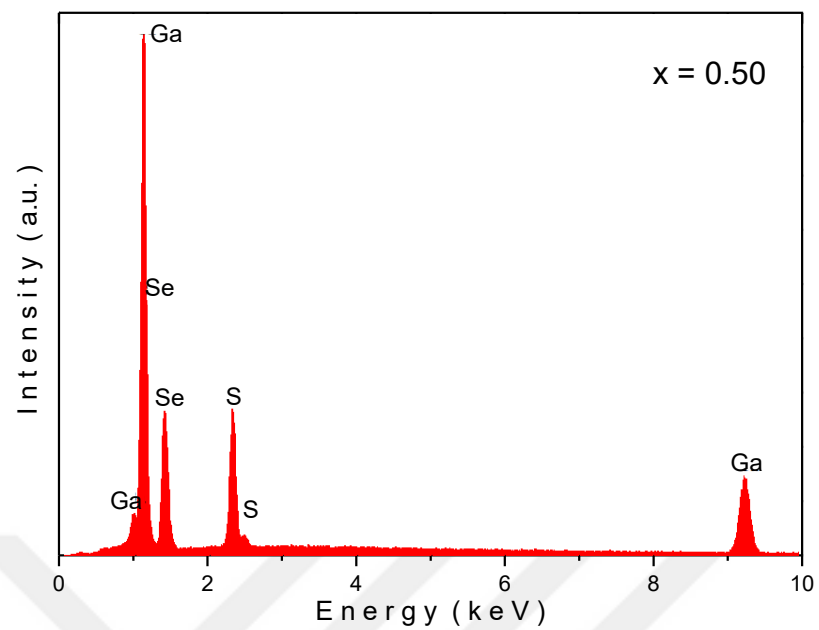
CHAPTER IV

RESULTS AND DISCUSSION

4.1 Results of Energy Dispersive Spectroscopy Analyses

The chemical composition of the studied crystals were determined using energy dispersive spectroscopy analyses technique. Fig. 4.1 shows the energy dispersive spectra of $\text{GaS}_x\text{Se}_{1-x}$ mixed crystals for composition x increasing from 0 (GaSe) to 1 (GaS) by intervals of 0.25 and in the energy range of 0-10 keV. The emission energies are characteristic properties of an element. These energies are reported for Ga, S and Se elements as (1.098, 1.125, 1.144, 1.171 and 9.241 keV), (0.163, 0.164, 2.307, 2.464 and 2.470 keV) and (1.379, 1.419, 1.434 and 1.475 keV), respectively [45]. As can be observed from the figures, some of these characteristic energies seem in the spectra. The variation of selenium/sulfur composition in the mixed crystals show itself in the spectra by comparison of mainly two peaks. The intensity of peak around 1.38 keV associated with selenium decreases and intensity of peak around 2.30 keV associated with sulfur increases as sulfur composition (x value) increases in the $\text{GaS}_x\text{Se}_{1-x}$ mixed crystals. Table 4.1 indicates the atomic composition ratios of involved elements in the mixed compounds. These ratios are well matched with the x values increasing from 0 to 1 by intervals of nearly 0.25.





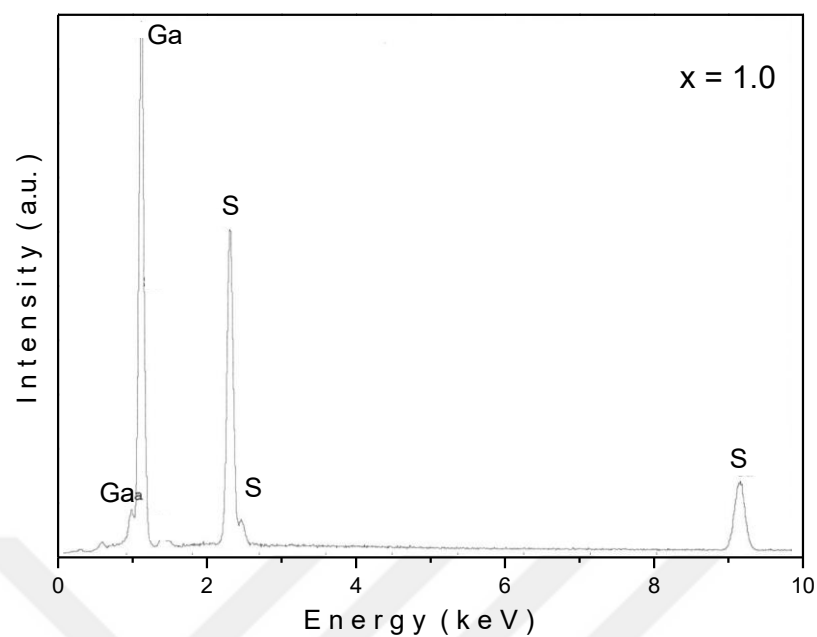


Figure 4.1 Energy dispersive spectra of $\text{GaS}_x\text{Se}_{1-x}$ mixed crystals

Table 4.1. EDS results for $\text{GaS}_x\text{Se}_{1-x}$ mixed crystals.

x	Sample	Ga %	Se %	S %
0	GaSe	49.2	50.8	0
0.25	$\text{GaS}_{0.25}\text{Se}_{0.75}$	50.4	37.4	12.2
0.50	$\text{GaS}_{0.5}\text{Se}_{0.5}$	49.8	25.4	24.8
0.75	$\text{GaS}_{0.75}\text{Se}_{0.25}$	51.0	12.2	36.8
1.0	GaS	52.8	0	47.2

4.2 Results of X-ray Diffraction

$\text{GaS}_x\text{Se}_{1-x}$ mixed crystal were structurally characterized by XRD experiments. XRD measurements were accomplished for the incident angle range of $10\text{-}90^\circ$ to understand the crystalline quality and obtain lattice parameters. Fig. 4.2 presents the

diffraction patterns of studied mixed crystals. As can be concluded from sharp peaks, all samples grew successfully in single crystal form. The diffraction angle values of mixed compounds are observed between those of constituent compounds of GaSe and GaS. For example, most intensive peaks of GaSe and GaS appear at angles (2θ) of 22.32° and 22.93° , respectively. The same peak was observed for $\text{GaS}_x\text{Se}_{1-x}$ mixed crystals at 22.28° ($x = 0.25$), 22.44° ($x = 0.50$) and 22.60° ($x = 0.75$). This behavior is generally observed for other peaks in the diffraction patterns. Under the light of this shift behavior, observed peaks are associated with each other and given in Table 4.2. There are some missing parts in association of diffraction angles. This is most probably due to the fact that possible configuration is not positioned when powder is placed into device or number of parallel planes of corresponding angles is not enough to present peak in the XRD pattern. It is known that parallel planes around 10^3 - 10^5 produce sufficient XRD peaks in the experiments. The crystal system and lattice parameters were calculated using a software program named as "TREOR 90". Analyses resulted with crystal system of hexagonal structure for all studied samples. This result shows good consistency with reported crystal structure of $\text{GaS}_x\text{Se}_{1-x}$ mixed crystals for x values of $0 \leq x \leq 0.5$ [31].

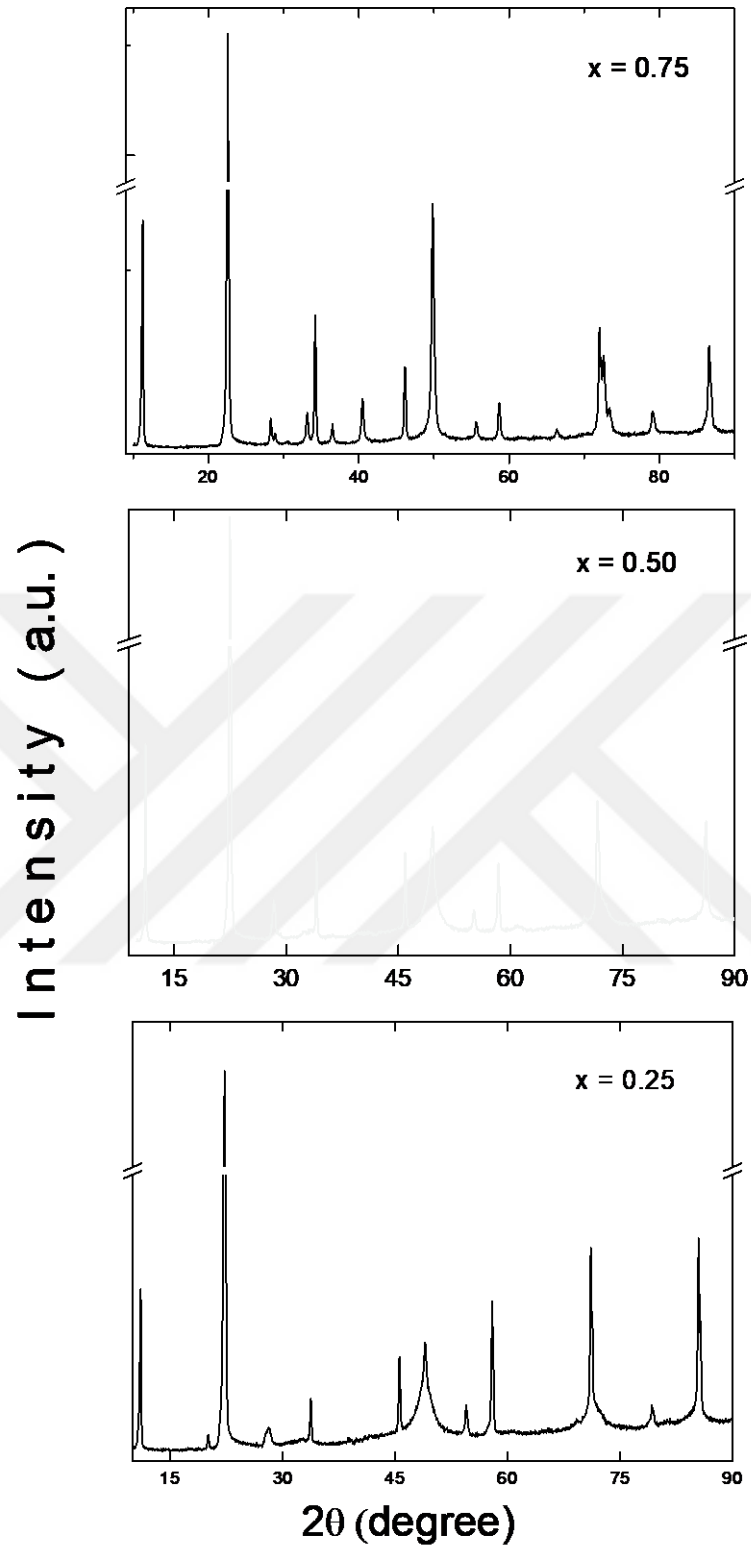


Figure 4.2 X-ray powder diffraction patterns of GaS_xSe_{1-x} mixed crystals

Table 4.2 Positions (2θ) of observed diffraction peaks in XRD patterns

2θ (Degree)				
$x = 0^*$	$x = 0.25$	$x = 0.50$	$x = 0.75$	$x = 1.0^{**}$
11.10	11.05	11.16	11.23	11.41
22.32	22.28	22.44	22.60	22.93
28.02	28.10	28.29	28.33	28.73
—	—	—	28.85	29.31
32.29	—	—	33.15	33.65
33.75	33.76	33.92	34.20	34.69
35.65	—	—	36.51	37.07
39.60	—	—	40.51	41.11
45.54	45.59	45.87	46.15	46.85
48.84	48.99	49.61	49.79	50.59
54.02	54.50	55.12	55.64	55.89
56.63	57.96	58.40	58.71	59.50
65.21	—	—	66.36	67.41
70.98	71.07	71.59	72.04	73.21
71.30	—	—	72.58	73.78
78.80	79.32	—	—	82.05
84.53	85.50	86.14	86.62	87.58

* Ref. [46]

** Ref. [47]

The lattice parameters were reported for GaSe as $a = 0.375$ nm, $c = 1.592$ nm and for GaS as $a = 0.3585$ nm, $c = 1.550$ nm [46, 47]. The lattice parameters of mixed crystals decreases as sulfur concentration is increased. Fig. 4.3 presents the compositional variation of lattice parameters. These plots can be fitted under the light

of Vegard-like function with linear interpolation. The linear fit resulted with functions of $a(x) = 0.37524 - 0.01652x$ (nm) and $c(x) = 1.59794 - 0.04548x$ (nm). The increase of lattice parameters with increase of bigger anion or cation was also observed previously in literature on the $K_{1-x}Rb_xTiOPO_4$, $KCl_{1-x}Br_x$, $TlGa(S_{1-x}Se_x)_2$, $TlIn_{1-x}Ga_xSe_2$, $TlGa_{1-x}In_xS_2$ and $TlIn(Se_{1-x}S_x)_2$ mixed crystals [48-50]. When the bigger atom (Se) replaces the smaller atom (S), lattice expansion in the mixed crystals is observed.

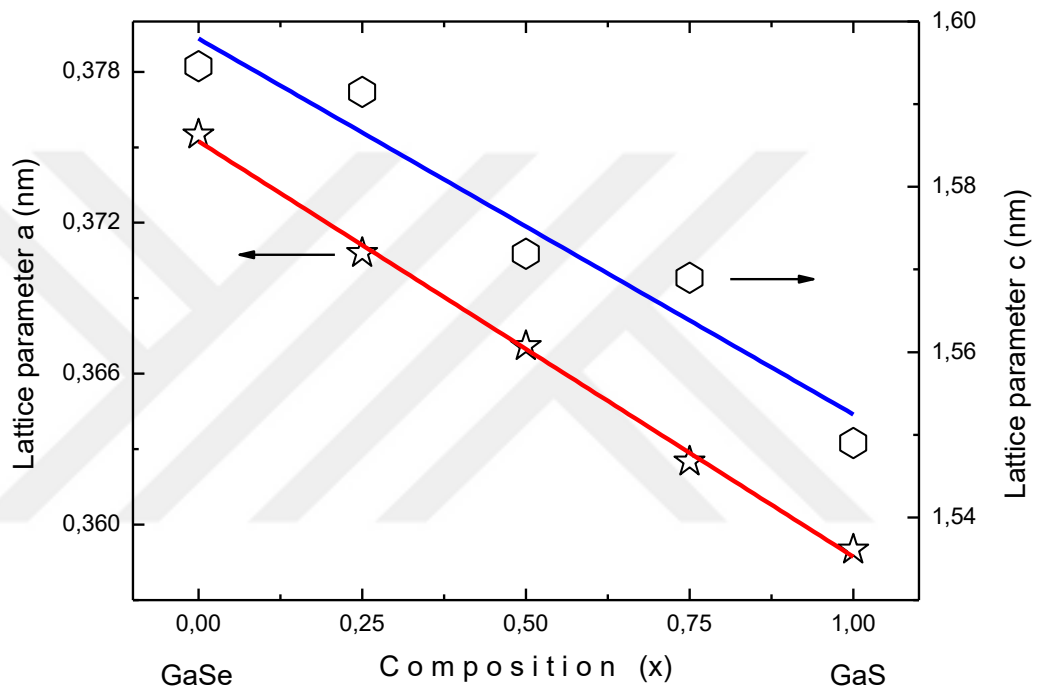
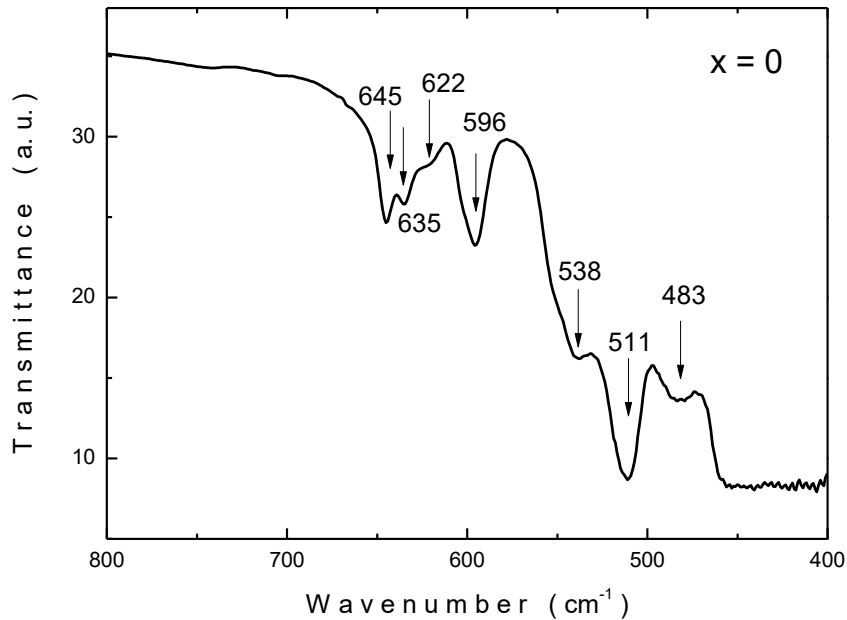


Figure 4.3 Compositional dependence of lattice parameters

4.3. Results of Fourier Transform Infrared Spectroscopy Measurements

Fig. 4.4 indicates the infrared transmittance spectra of $\text{GaS}_x\text{Se}_{1-x}$ mixed crystal for compositions of $x = 0, 0.25$ and 0.50 . Due to thickness problem of compositions $x = 0.75$ and 1.0 , transmittance spectra were not clear and therefore not presented. As given also in Table 4.3 infrared spectra of GaSe , $\text{GaS}_{0.25}\text{Se}_{0.75}$ and $\text{GaS}_{0.5}\text{Se}_{0.5}$ presented seven, two and four minima positions, respectively. These minima positions are considered due to the multiphonon absorption. In literature, there are two reports concerning the optical phonons and two phonon absorption in the studied crystals. Gasanly et al. measured the Raman scattering and infrared reflection spectra of $\text{GaS}_x\text{Se}_{1-x}$ mixed crystal [51]. Riede et al. reported the optical transmission spectra of GaSe in the spectral range of $180\text{-}600\text{ cm}^{-1}$ [52] and attributed the observed peaks to two phonon combination modes. Under the light of these two studies, observed peaks were interpreted to multiphonon absorption. Table 4.3 presents proposed assignments of each observed peak in infrared spectra. It can be seen from the proposed assignments that there exist multiphonon absorptions in the crystals.



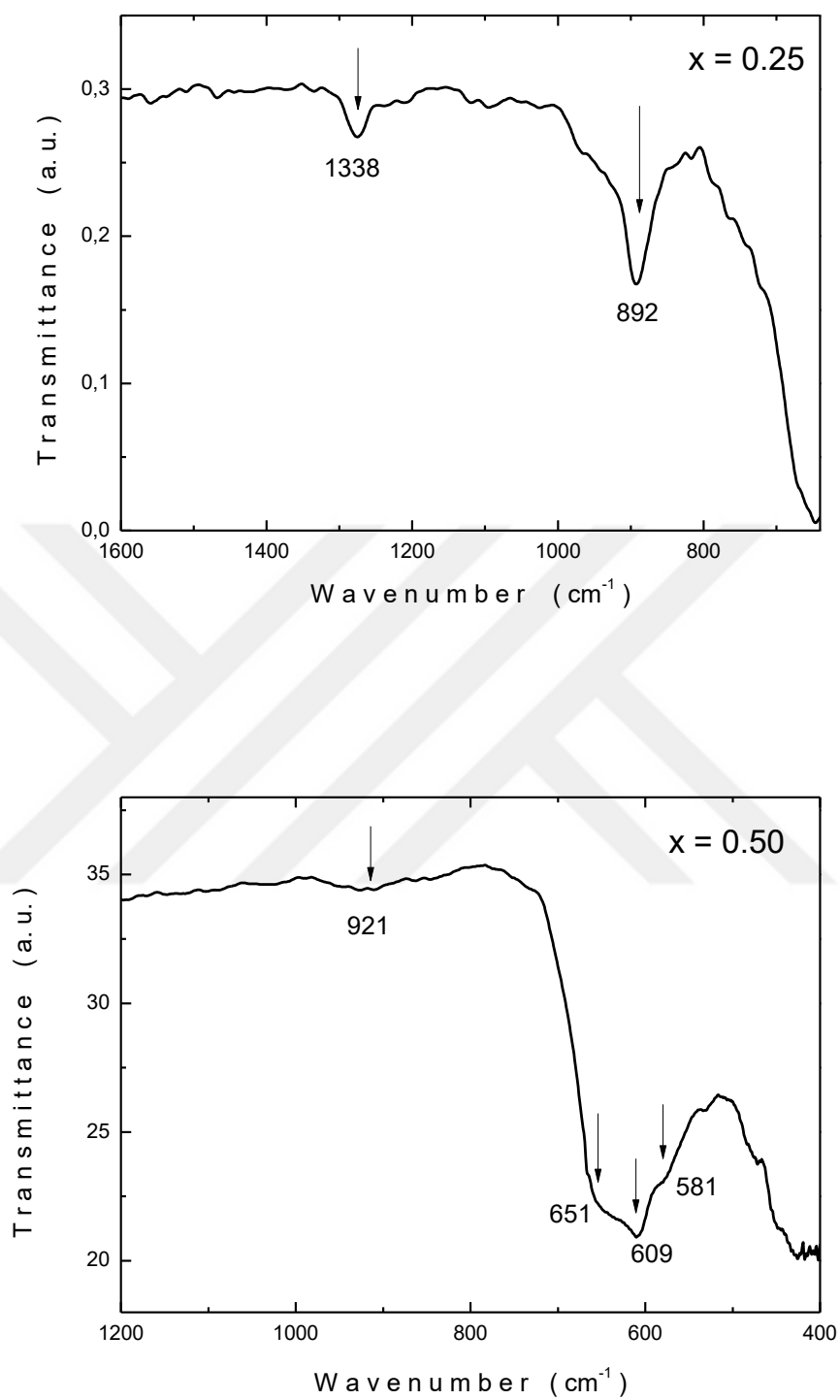


Figure 4.4 Infrared transmittance spectra of GaS_xSe_{1-x} mixed crystals

Table 4.3 The frequencies (cm^{-1}) reported previously by different methods and observed in infrared transmittance spectra.

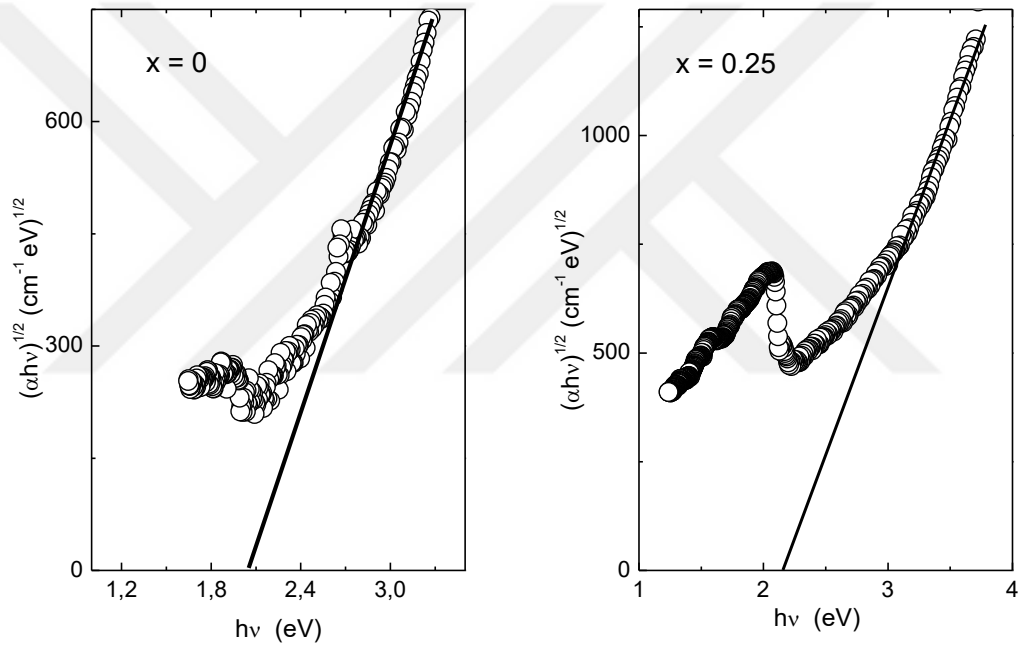
$x = 0$ (GaSe)			
Raman scattering [53]	IR reflectivity Ref. [52]	IR transmittance (this work)	Proposed assignment
—	19	483	$237 + 246 = 483$
—	37	511	$255 \times 2 = 510$
59	60	538	$237 \times 2 + 60 = 534$
134	134	596	$37 + 246 + 309 = 592$
—	212	622	$308 \times 2 = 616$
213	214	635	$212 \times 3 = 636$
—	237	645	$214 \times 3 = 642$
—	246		
253	255		
308	309		

	IR reflectivity* [51]	IR transmittance (this work)	Proposed assignment
$x = 0.25$ (GaS _{0.25} Se _{0.75})	~ 295	892	$295 \times 3 = 885$
	~ 315	1273	$315 \times 4 = 1260$
$x = 0.50$ (GaS _{0.5} Se _{0.5})	~ 315	581	$290 \times 2 = 580$
	~ 290	609	$315 + 290 = 605$
	~ 216	651	$216 \times 3 = 648$
		921	$315 \times 2 + 290 = 920$

*In Ref. [51], infrared reflectivity spectra of the crystals are given. Paper does not give any frequency value. Since values are read using reported plot, we give approximate frequency values.

4.4 Results of Ellipsometry Measurements

Ellipsometric measurements were applied on $\text{GaS}_x\text{Se}_{1-x}$ mixed crystals at room temperature. The output data, ψ and Δ , were analyzed to calculate extinction coefficient of the samples using air/sample optical model which is suitable model for bulk crystals. Extinction coefficient gives opportunity to obtain absorption coefficient (α) using Eq. 2.10. Band gap energies of the studied samples can be estimated analyzing the spectral dependence of absorption coefficient in the absorption edge region using Eq. 2.11. For this purpose, $(\alpha h\nu)^{1/2}$ vs. $(h\nu)$ plots were drawn as shown in Fig. 4.5.



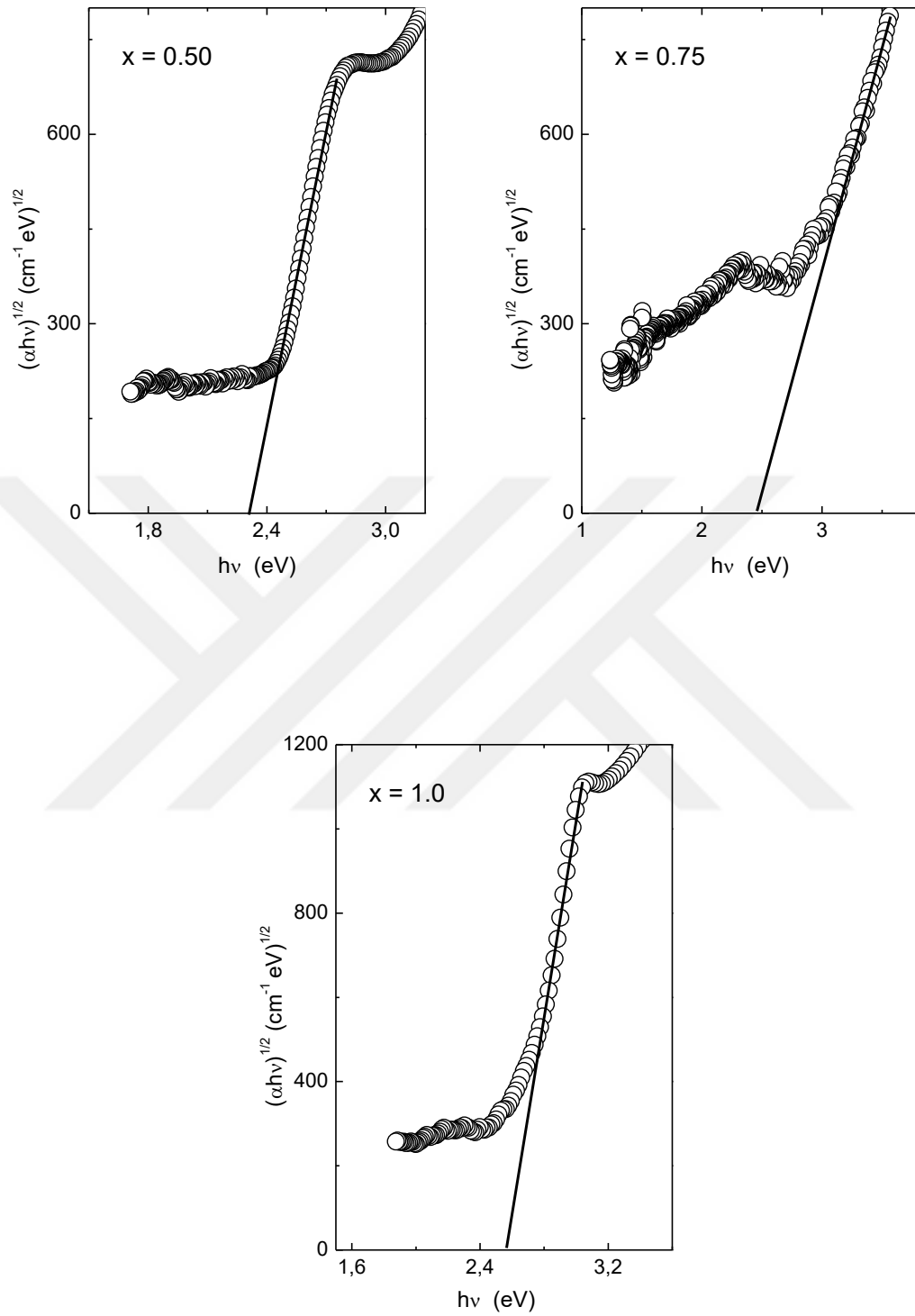


Figure 4.5 $(\alpha h\nu)^{1/2}$ vs. $(h\nu)$ plots of GaS_xSe_{1-x} mixed crystals

Eq. 2.11 indicates that intersection point of fitted line on the $h\nu$ -axis when $(\alpha h\nu)^{1/2}$ is equal to 0 gives indirect band gap energy of studied crystals. In each graph, fitted lines and intersection points on the $h\nu$ -axis are presented. Table 4.4 shows obtained energy values of present study and previously reported values revealed using different experimental techniques. As can be seen from the table, band gap energy increases with increase of sulfur concentration in the mixed crystals. This behavior indicated that gap energy increases when smaller anion or cation concentration increases. In the literature, similar behavior was also observed on $Al_xGa_{1-x}P$, $Ge_{1-y}Sn_y$ and $Ga_xIn_{1-x}Se$ mixed compounds [54-56].

Table 4.4 Band gap energy values (eV) of GaS_xSe_{1-x} mixed crystals and fitting parameters according to Eq. 4.1

	Method		
	Ellipsometry (Present study)	Transmission Reflection Ref. [34]	Absorption Piezoreflectance Ref. [31]
$x = 0$	2.04	1.99	1.986
$x = 0.25$	2.15	2.13	2.16
$x = 0.50$	2.31	2.24	2.37
$x = 0.75$	2.44	2.39	—
$x = 1$	2.57	2.55	—
$E(0)$	2.033	1.994	1.986
b	0.53	0.51	0.62
c	0.011	0.046	0.26

Band gap energies of GaSe, GaS and GaS_xSe_{1-x} mixed crystals were reported from different optical characterization techniques. The indirect band gap of constituent compounds, GaSe and GaS, were found as 1.989 and 2.5 eV, respectively [25,31]. When these values were compared with our results, a very good consistency can be seen between values. In the literature, there are two papers concerning band gap calculation of GaS_xSe_{1-x} mixed crystals. Isik et al. reported the band gap energies of mixed crystals in the compositional range of $0 \leq x \leq 1$ by $x = 0.25$ intervals using transmission and reflection experiments [34]. Wu et al. obtained the gap energies for

compositional range of $0 \leq x \leq 1$ by $x = 0.1$ intervals using absorption and piezoreflectance measurements [31]. Derivative spectrophotometry method applied on transmission and reflection spectra showed that band gap energy increases from 1.99 eV ($x = 0$) to 2.55 eV ($x = 1$) [34] and absorption, piezoreflectance analyses presented that gap energy increases from 1.986 eV ($x = 0$) to 2.37 eV ($x = 0.5$) [31] (see Table 4.4). The results of ellipsometric measurements to obtain band gap energy show good agreement with reported values.

In Ref. [57], band gap energy (E_g)-composition (x) dependency was expressed by the relation

$$E(x) = E(0) + bx + cx^2 \quad (4.1)$$

where $E(0)$ and b parameters are decided from gap energies of pure semiconductor materials and c symbolize bowing parameter. Fig. 4.6 shows the compositional dependency of band gap energy and fitted line obtained under the light of Eq. 4.1. Outputs of fitting process are $E(0) = 2.033$ eV, $b = 0.53$ eV and $c = 0.011$ eV. This analyses were also applied in Refs. [31,34]. The results of these papers are also indicated in Table 4.4.

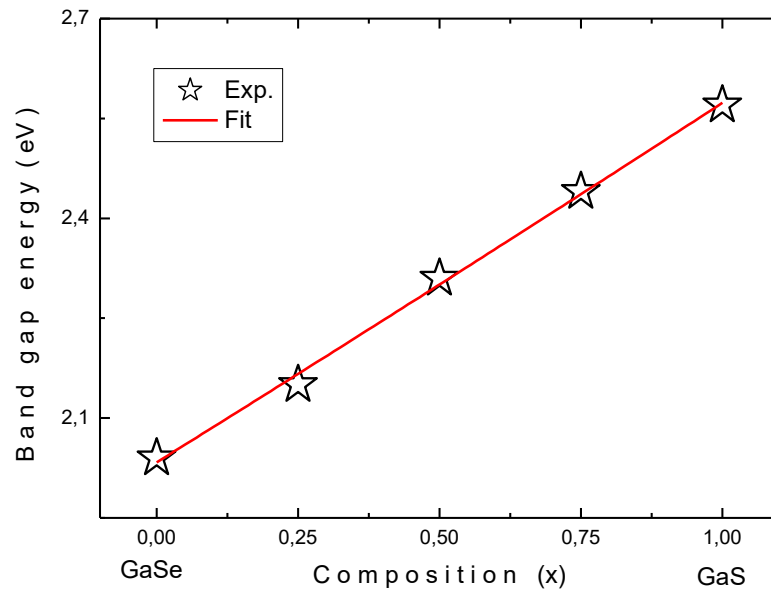


Figure 4.6 Compositional dependence of band gap energies (stars) and fitted line according to Eq. 4.1

CHAPTER V

CONCLUSION

Structural and optical characterization techniques were used to investigate GaS_xSe_{1-x} layered mixed crystals. Chemical composition of used samples grown by Bridgman method were determined using energy dispersive spectroscopic analyses method. It was shown that composition x varies from 0 (GaSe) to 1 (GaS) by intervals of 0.25. The used compositions gave a very big possibility to us to understand how the investigated structural and optical parameters vary as sulfur or selenium composition is changed in the mixed crystals. X-ray diffraction method was used to get information about the crystalline structure of the used semiconducting crystals. Analyses resulted with crystal system of hexagonal structure for all studied samples. The analyses indicated that lattice parameters of the crystal decreases from $a = 0.375$ nm (GaSe) to $a = 0.3585$ nm (GaS) and $c = 1.592$ nm (GaSe) to $c = 1.550$ nm (GaS) as sulfur concentration is increased. Compositional dependence of revealed lattice parameters was plotted and nearly a linear behavior was observed. The increase of lattice parameters with increase of bigger atom indicated us that there exist a lattice expansion in mixed crystals with increase of selenium atom. Infrared transmittance spectra of mixed crystals for $x = 0, 0.25$ and 0.50 were obtained from FTIR measurements. The observed minima positions in each crystal were attributed to multiphonon absorption under the light of results of Raman and infrared reflectivity measurements previously reported in literature. According to reported phonon frequency values, observed minima positions were successfully related to two and three multiphonon absorptions.

Ellipsometry measurements were used for optical characterization of the samples. The output data of the used ellipsometry device were converted to optical

parameters using suitable optical models. Then spectra of absorption coefficient were obtained. This plot was used to find the band gap energy of the samples. The analyses indicated that band gap energy increases from 2.04 eV (GaSe) to 2.57 eV (GaS) as sulfur concentration is increased in the mixed crystals. Compositional dependence of band gap energy was analyzed using second order polynomial expression defined for semiconductor materials. All revealed results were compared with similar results obtained from different techniques.



REFERENCES

- [1] V. Capozzi, Phys Rev B 28 (1983) 4260.
- [2] A. Kuhn, A. Chevy, R. Chevalier. Phys. Stat. Sol. (a) 31 (1975) 469.
- [3] T. Tambo, C. Tatsuyama, Surface Science 222 (1989) 343.
- [4] K. Uneo, K. Saiki, A. Koma, Jap. J. Appl. Lett.30 (1991) L1352.
- [5] D.V. Rybkovskiy, A.V. Osadchy, E.D. Obraztsova, Phys. Rev. B 90 (2014) 235302.
- [6] O. Karabulut, *Structural, Electrical and Optical Characterization of N- and Si-implanted GaSe Single Crystal Grown by Bridgman Method*, Ph.D Thesis, Middle East Technical University, 2003.
- [7] E. Aulich, J.L. Brebner, E. Mooser, Phys. Stat. Sol. (b) 31 (1969) 129.
- [8] M.K. Anis, J. Crys. Growth 55 (1981) 465.
- [9] S.G. Choi, D.H. Levi, C. Martinez-Tomas, V.M. Sanjose, J. Appl. Phys. 106 (2009) 053517.
- [10] M. Isik, E. Tugay, N.M. Gasanly, Philos. Magazine 96 (2016) 2564.
- [11] N.M. Gasanly, A. Aydinli, O. Salihoglu, Cryst. Res. Technol. 36 (2001) 295.
- [12] M. Isik, W. Hadibrata, N.M. Gasanly, J. Lumin. 154 (2014) 131.
- [13] A.Aydınlı, N.M. Gasanly, K. Goksen, Phil. Mag. Lett. 81 (2001) 859.
- [14] A. Seyhan, O. Karabulut, B.G. Akınođlu, B. Aslan, R. Turan, Cryst. Res. Technol. 40 (2005) 893.
- [15] S. Shigetomi, T. Ikari, J. Appl. Phys. 88 (2000) 1520.
- [16] Y. Iwamura, M. Moriyama, N. Watanabe, Jpn. J. Appl. Phys. 30 (1991) L42.

- [17] N.B. Singh, D.R. Suhre, V. Balakrishna, M. Marable, R. Meyer, N. Fernelius, F.K. Hopkins, D. Zelmon, *Progress in Crystal Growth and Characterization of Materials* 37 (1998) 47.
- [18] G.B. Abdullaev, K.R. Allakhverdiev, M.E. Karasev, V.I. KOnov, L.A. Kulevskii, N.B. Mustafaev, P.P. Pashinin, A.M. Prokhorov, Yu. M. Starodumov, N.I. Chapliev, *Sov. J. Quantum Electron* 19 (1989) 494.
- [19] D.J. Late, B. Liu, J. Luo, A. Yan, H.S.S.R. Matte, M. Grayson, C.N.R. Rao, V.P. Dravid, *Adv. Mater.* 24 (2012) 3549.
- [20] A.G. Kyazym-zade, A.A. Agaeva, V.M. Salmanov, A.G. Mokhtari, *Tech. Phys.* 52 (2007) 1611.
- [21] M. Balkanski and R.F. Wallis, *Semiconductor Physics and Applications Oxford University Press*, New York (2000).
- [22] Z. Zhu, Y. Cheng, U. Schwingenschloegl, *Phys. Rev. Lett.* 108 (2012) 266805.
- [23] F. Levy, *Crystallography and Crystal Chemistry of Materials with Layered Structures*, Reidel, Dordrecht (1976).
- [24] E. Aulich, J.L. Brebner, E. Mooser, *Phys. Status Solidi* 31 (1969) 129.
- [25] C.H. Ho, S.L. Lin, *J. Appl. Phys.* 100 (2006) 083508.
- [26] M. Isik, E. Tugay, N. Gasanly, *Indian J. Pure & Appl. Phys.* 55 (2017) 583.
- [27] M. Isik, N.M. Gasanly, R. Turan, *Physica B* 408 (2013) 43.
- [28] A. Aydinli, N.M. Gasanly, K. Goksen, *J. Appl. Phys.* 88 (2000) 7144.
- [29] N.M. Gasanly, A. Aydinli, N.S. Yuksek, O. Salihoglu, *Appl. Phys. A* 77 (2003) 603.
- [30] S. Delice, E. Bulur, N.M. Gasanly, *Philos. Mag.* 95 (2015) 998.
- [31] C.C. Wu, C.H. Ho, W.T. Shen, Z.H. Cheng, Y.S. Huang, K.K. Tiong, *Mater. Chem. Phys.* 88 (2004) 313.
- [32] C.H. Ho, C.C. Wu, Z.H. Cheng, *J. Cryst. Growth* 279 (2005) 321.
- [33] M. Isik, N.M. Gasanly, *Opt. Mater.* 54 (2016) 155.
- [34] M. Isik, N.M. Gasanly, *Mat. Chem. Phys.* 190 (2017) 74.
- [35] R. de L. Kronig, W. G. Penney, *Proc. Roy. Soc. (London)* A130 (1930) 499.

- [36] C. Kittel, *Introduction to Solid State Physics*, John Wiley & Sons, New York (2005).
- [37] B. G. Yacobi, *Semiconductor Materials; An Introduction to Basic Principles*, Kluwer Academic, New York (2003).
- [38] W. L. Bragg, Proceedings of the Royal Society of London Series A 17, Part I, (1913) 43.
- [39] M. Uo, T. Wada, T. Sugiyama, *Jpn. Dent. Sci. Rev.* 51 (2015) 2.
- [40] H. Fujiwara, *Spectroscopic Ellipsometry Principles and Applications*, John Wiley & Sons, New York (2007).
- [41] J. I. Pankove, *Optical Processes in Semiconductors*, Prentice Hall, New Jersey (1971).
- [42] T. S. Moss, G. J. Burrell and B. Ellis, *Semiconductor Opto-Electronics*, John Wiley & Sons, New York (1973).
- [43] <https://www.britannica.com/technology/scanning-electron-microscope>
- [44] <http://lipidlibrary.aocs.org/Biochemistry/content.cfm?ItemNumber=40299>
- [45] J. Goldstein, D. Newbury, D. Joy, C. Lyman, P. Echlin, E. Lifshin, L. Sawyer, J. Michael, *Scanning Electron Microscopy and X-Ray Microanalysis*, Springer Science, LLC, New York (2007).
- [46] JCPDS (Joint Committee on Powder Diffraction Standart) Card no: 65-3507.
- [47] JCPDS (Joint Committee on Powder Diffraction Standart) Card no: 65-1980.
- [48] R. Kriegel, R. Wellendorf, C. Kaps, *Mat. Res. Bulletin* 36 (2001) 245.
- [49] F. Samavat, E. Haji-Ali, S. Shahmaleki, S. Solgi, *Adv. Mater. Phys. Chem.* 2 (2012) 85.
- [50] N.M. Gasanly, *Indian J. Phys.* 89 (2015) 657.
- [51] N.M. Gasanly, A.F. Goncharov, N.M. Melnik, A.S. Ragimov, *Phys. Stat. Sol. (b)* 120 (1983) 137.
- [52] V. Riede, H. Neumann, F. Levy, H. Sobotta, *Phys. Stat. Sol. (b)* 104 (1981) 277.
- [53] K. Allakhverdiev, T. Baykara, S. Ellialtioglu, F. Hashimzade, D. Huseinova, K. Kawamura, A.M. Kulibekov, S. Onari, *Mater. Res. Bull.* 41 (2006) 751.

[54] S.G. Choi, Y.D. Kim, S.D. Yoo, D.E. Aspnes, D.H. Woo, S.H. Kim, J. Appl. Phys. 87 (2000) 1287.

[55] L. Jiang, J.D. Gallagher, C.L. Senaratne, T. Aoki, J. Mathews, J. Kouvetakis, J. Menendez, Semicond. Sci. Technol. 29 (2014) 1150258.

[56] L. Gousskov, A. Gousskov, M. Hajjar, L. Soonckindt, C. Llinares, Physica B 99, (1980) 291.

[57] J.A. Van Vechten, T.K. Bergstresser, Phys. Rev. B 1 (1970) 3351.

